NASA Contractor Report 182051

ICASE Report No. 90–40

ICASE

ON THE INSTABILITY OF HYPERSONIC FLOW PAST A FLAT PLATE

Nicholas Blackaby
Stephen Cowley
Philip Hall

Contract No. NAS1–18605
May 1990

Institute for Computer Applications in Science and Engineering
NASA Langley Research Center
Hampton, Virginia 23665–5225

Operated by the Universities Space Research Association

National Aeronautics and
Space Administration

Langley Research Center
Hampton, Virginia 23665-5225

ON THE INSTABILITY OF HYPERSONIC FLOW PAST A FLAT PLATE[1]

Nicholas Blackaby
Mathematics Department
Exeter University, Exeter EX4 4QE
United Kingdom

Stephen Cowley
Mathematics Department
Imperial College, London SW7 2BZ
United Kingdom

Philip Hall
Mathematics Department
Exeter University, Exeter EX4 4QE
United Kingdom

ABSTRACT

The instability of hypersonic boundary-layer flows over flat plates is considered. The viscosity of the fluid is taken to be governed by Sutherland's law, which gives a much more accurate representation of the temperature dependence of fluid viscosity at hypersonic speeds than Chapman's approximate linear law; although at lower speeds the temperature variation of the mean state is less pronounced so that the Chapman law can be used with some confidence. Attention is focussed on the so-called "vorticity" mode of instability of the viscous hypersonic boundary layer. This is thought to be the fastest growing *inviscid* disturbance at hypersonic speeds; it is also believed to have an asymptotically larger growth rate than any viscous or centrifugal instability. As a starting point we investigate the instability of the hypersonic boundary layer which exists far downstream from the leading edge of the plate. In this regime the shock that is attached to the leading edge of the plate plays no role, so that the basic boundary layer is non-interactive. It is shown that the vorticity mode of instability of this flow operates on a significantly different lengthscale than that obtained if a Chapman viscosity law is assumed (see Smith and Brown, 1989). In particular, we find that the growth rate predicted by a linear viscosity law overestimates the size of the growth rate by $O(M^2)$. Next, the development of the vorticity mode as the wavenumber decreases is described, and it is shown that acoustic modes emerge when the wavenumber has decreased from it's $O(1)$ initial value to $O(M^{-\frac{8}{3}})$. Finally, the inviscid instability of the boundary layer near the leading edge in the interaction zone is discussed and particular attention is focussed on the strong interaction region which occurs sufficiently close to the leading edge. We find that the vorticity mode in this regime is again unstable, and that it is concentrated in the transition layer at the edge of the boundary layer where the temperature adjusts from its large, $O(M^2)$, value in the viscous boundary layer, to its $O(1)$ free stream value. The existence of the shock indirectly, but significantly, influences the instability problem by modifying the basic flow structure in this layer.

[1]Research was supported by the National Aeronautics and Space Administration under NASA Contract No. NAS1-18605 while the authors were in residence at the Institute for Computer Applications in Science and Engineering (ICASE), NASA Langley Research Center, Hampton, VA 23665.

1. INTRODUCTION

Our concern is with the inviscid mode of instability of hypersonic boundary-layer flows over flat plates. In the first instance we will consider a regime where there are no shocks present, and then we will show how the instability problem is significantly modified by the presence of a shock in the flow field. The motivation for this and related work on hypersonic boundary-layer instability theory is the renewed interest in hypersonic flight which has been stimulated by plans to build a successor to the Space Shuttle. A primary concern with such a vehicle is the question of where transition will occur over a wide range of Mach numbers and whether it can be controlled. At the largest relevant Mach numbers, say Mach 20-25, the extremely high temperatures associated with the flow would destroy the vehicle unless it were cooled, so that it is of interest to know the effect of the wall temperature on the instability properties of the flow. The purpose of this paper is to determine the inviscid instability characteristics of physically realistic hypersonic boundary-layer flows. We note here in passing that there is a simple generalization of Rayleigh's (incompressible) inflection point theorem to compressible flows (Lees & Lin, 1946), and that many compressible boundary layers turn out to be inviscidly unstable even though their incompressible counterparts are stable. This is a significant result because the growth rates of inviscid disturbances are generally much larger than those of viscous or centrifugal instabilities so that they are the likely cause of transition to turbulence in most situations. The modes which we discuss in this paper can be referred to as generalized inflection point modes because, when neutral, their phase speed is equal to the fluid velocity at the generalized inflection point. Furthermore the eigenfunctions of the modes are localized around that point.

For convenience we will concentrate on high-Reynolds-number flow past a flat plate, although many aspects of our analysis are applicable to other boundary-layer flows (e.g. flow past a wedge). The underlying steady flows that we study depend upon the Mach number, the Prandtl number and the choice of the viscosity law; the complications arising from real gas effects are not investigated. Throughout we assume that the fluid viscosity is Newtonian and is adequately described by Sutherland's formula. We will also take the Prandtl number to be one, noting that it is relatively straightforward to relax this restriction. Moreover the relaxation of the latter restriction does not significantly alter the qualitative features of the results we present here.

Reshotko (1976) and Mack (1987) have reviewed earlier work on the linear instability of high-Reynolds-number compressible flows. Many of these studies are based on the Orr-Sommerfeld equation; for a critique of the mathematical rigor of this approach see Smith (1979, 1989). Here we examine the linear stability of high-Reynolds-number flows by means of formal asymptotic expansions; for example Smith (1989) has applied triple-deck theory to the lower-branch viscous Tollmien-Schlichting modes of compressible boundary layers. Seddougui, Bowles & Smith (1989) have extended this theory to include the effects of severe wall cooling, while Cowley & Hall (1988) have shown how such modes can interact with a shock at large Mach number. However, the viscous modes have relatively small growth rates, and our main concern here will be with inviscid modes. The nature of the asymptotic expansion procedure in these investigations clearly depends on the nature of the mode of instability. In fact the third type of instability responsible for boundary-layer transition, the Görtler vortex mode, develops an asymptotic structure at high Mach numbers closely related to that found here; see Hall and Fu (1989).

When a quasi-parallel approximation is formally justifiable because the Reynolds number is large, inviscid modes satisfy the compressible Rayleigh equation. Numerical solutions to this equation have been reported by, *inter alia*, Mack (1984, 1987) for boundary-layer flows, Grosch & Jackson (1989) for shear flows, and Papageorgiou (1989) for wake flows. For fluids satisfying a Chapman viscosity law, high-Mach-number asymptotic solutions to this equation for the so-called "acoustic" boundary-layer modes have been obtained by Cowley & Hall (1989), while Smith & Brown (1989) have identified the asymptotic form of the "vorticity" mode. Goldstein & Balsa (1989) have given an asymptotic solution for high-Mach-number, shear-layer modes of instability for a Chapman fluid. Though the basic states investigated by the two latter pairs of authors are different, they found essentailly the same most unstable eigenvalue because it corresponds to a disturbance trapped in a thin layer where the overall features of the basic state are unimportant. However Goldstein and Balsa did not spot the exact solution of the vorticity mode equation found by Smith and Brown.

Both in the above mentioned boundary-layer analyses, and the hypersonic Görtler vortex instability analysis of Hall & Fu (1989), one of the key asymptotic regions for the case of a Chapman viscosity law is a *logarithmically* thin layer which develops due to the *exponential* decay of the underlying steady temperature field away from the wall. However, Chapman's viscosity law is not exact, and was introduced as a useful interpolation law

which greatly simplified steady boundary-layer calculations (e.g. see Stewartson 1964). At the large temperatures typical in hypersonic flows, it differs significantly from the more precise Sutherland's formula. In fact Chapman's law is simply a linear approximation to the viscosity-temperature dependence of the fluid; it is therefore of questionable validity in the hypersonic limit. At high Mach numbers the steady temperature field in a fluid satisfying Sutherland's formula initially decays algebraically away from the wall, before reverting to exponential decay in an asymptotic region "far" from the wall (e.g. Freeman & Lam 1959). The effect of this algebraic decay is to change significantly the scalings in the transition region; in particular the asymptotic expansions proceed in inverse powers of M rather than $\sqrt{\log(M)}$. Moreover the wavelength of the most unstable disturbance varies by a factor of $\sqrt{\log(M)}$ in the two cases. We note that a similar difference in scalings is evident in the interaction region of steady hypersonic flow past a flat plate. In that case Lee & Cheng (1969) have shown that the shock-heating transition layer is logarithmically thin for Chapman's viscosity law, whereas for a power-law viscosity formula, and hence for Sutherland's formula, the scaling for the transition layer is algebraic (Bush 1966).

The flows which we consider here are appropriate to different stages of hypersonic flow past a semi-infinite flat plate. In the first instance we shall consider the instability of a non-interactive flow which is appropriate to large distances downstream of the leading edge of the plate. Here the attached shock at the leading edge has no effect on the flow field and the basic state is the Sutherland law counterpart of that discussed by Smith and Brown (1989). This basic state, and the Rayleigh equation which governs the inviscid instability, are discussed in Section 2. The dispersion relationship associated with this equation is then solved in Section 3. We shall discuss the growth rate of the mode over the whole range of unstable wavenumbers and discuss how the disturbance is related to the acoustic mode at small wavenumbers.

Then in Section 4 we go on to discuss the basic state in the so-called "strong interaction region" further upstream. The description of the basic flow in this regime for a power law fluid is due to Luniev (1959) and Bush (1966). We shall discuss how the interactive system for the flow can be formulated when the Mach number is of order $R^{\frac{1}{8}}$. However this system can only be solved numerically and we are not aware of any published results on that problem. Nevertheless we can of course still consider the instability of that state, and we derive the appropriate (quasi-parallel) stability equations in this regime. The strong hypersonic interaction limit then corresponds to taking the further limit of the

streamwise variable tending to zero. In that case a similarity solution for the basic flow can be found, Bush (1966), and a re-scaled Rayleigh equation for the disturbance is found. The solution of that equation is discussed in Section 5. We could have instead considered the weak hypersonic limit further downstream where Bush and Cross (1967) have given an appropriate asymptotic description. We choose to concentrate on the strong interaction regime because it is, to a certain extent, simpler. Further, if the flow is unstable in this regime it is likely that growing disturbances will originate here. Finally in Section 6 we shall draw some conclusions.

2. NON-INTERACTIVE STEADY FLOWS

We begin by considering the stability of steady hypersonic flow far downstream from any leading-edge interaction region; in particular, if L is the distance from the leading edge, and $\hat{U}_\infty$, $\hat{a}_\infty$, $\hat{\rho}_\infty$ and $\hat{\mu}_\infty$, are the velocity, sound speed, density and shear viscosity of the free stream flow, then we assume that the Reynolds number,

$$R = \frac{\hat{\rho}_\infty \hat{U}_\infty L}{\hat{\mu}_\infty} \tag{2.1a}$$

is larger than whatever power of the Mach number,

$$M = \frac{\hat{U}_\infty}{\hat{a}_\infty}, \tag{2.1b}$$

is necessary for interactive and/or non-parallel effects to be negligible (see below for a more precise restriction). We adopt a non-dimensionalisation based on coordinates $L\underline{x}$ (where x is in the direction of flow and y is normal to plate), velocities $\hat{U}_\infty \underline{u}$, time $Lt/\hat{U}_\infty$, pressure $\hat{\rho}_\infty \hat{U}_\infty^2 p$, density $\hat{\rho}_\infty \rho$, temperature $\hat{T}_\infty T$, and shear and bulk viscosities $\hat{\mu}_\infty \mu$ and $\hat{\mu}_\infty \mu'$ respectively, where the subscript ∞ denotes the value of the quantity in the free-stream. On the assumption that the fluid is a perfect gas with a constant ratio of specific heats γ, the governing equations of the flow are

$$\frac{\partial \rho}{\partial t} + \nabla \cdot (\rho \underline{u}) = 0, \tag{2.2a}$$

$$\rho \frac{D\underline{u}}{Dt} = -\underline{\nabla} p + \frac{1}{R}[2\nabla \cdot (\mu \underline{\underline{e}}) + \underline{\nabla}((\mu' - \frac{2}{3}\mu)\nabla \cdot \underline{u})], \tag{2.2b}$$

$$\rho \frac{DT}{Dt} = (\gamma - 1)M^2 \frac{Dp}{Dt} + \frac{1}{PrR}\nabla \cdot (\mu \underline{\nabla} T) + \frac{(\gamma - 1)M^2}{R}\Phi, \tag{2.2c}$$

$$\gamma M^2 p = \rho T, \tag{2.2d}$$

where

$$e_{ij} = \frac{1}{2}\left(\frac{\partial u_i}{\partial x_j} + \frac{\partial u_j}{\partial x_i}\right), \tag{2.3a}$$

$$\Phi = 2\mu \underline{\underline{e}} : \underline{\underline{e}} + (\mu' - \frac{2}{3}\mu)(\nabla \cdot \underline{u})^2, \tag{2.3b}$$

and Pr is the constant Prandtl number. For a shear viscosity obeying Sutherland's law

$$\mu = \left(\frac{1 + C}{T + C}\right) T^{\frac{3}{2}}, \tag{2.3c}$$

where $C \approx \dfrac{110.4}{\hat{T}_\infty}$ for air temperatures measured in degrees Kelvin. In the numerical calculations discussed in the next section we took $\hat{T}_\infty = 216.9$. The boundary-layer equation can be recovered by first substituting

$$\zeta = R^{\frac{1}{2}} \int_0^y \rho dy, \quad v = R^{-\frac{1}{2}} V, \tag{2.4a,b}$$

where the Dorodnitsyn-Howarth variable, ζ, is introduced for convenience, and then taking the limit $R \to \infty$.

For steady two-dimensional flow over a flat plate, a similarity solution to these equations exists. With

$$\eta = \frac{\zeta}{\sqrt{(1+C)x}}, \quad u = \psi_\zeta, \quad \rho V = -(\psi_x + \zeta_x \psi_\zeta), \tag{2.5a}$$

$$\psi = \sqrt{(1+C)x}\, f(\eta), \quad T \equiv T(\eta), \quad \rho \equiv \rho(\eta), \tag{2.5b}$$

the governing similarity equations are found to be

$$\rho T = 1, \tag{2.6a}$$

$$\frac{1}{2} f f'' + \left(\frac{T^{\frac{1}{2}}}{T+C} f'' \right)' = 0, \tag{2.6b}$$

$$\frac{1}{2} f T' + \frac{1}{Pr} \left(\frac{T^{\frac{1}{2}}}{T+C} T' \right)' + \frac{(\gamma-1)^2 M^2 T^{\frac{1}{2}}}{T+C} f''^2 = 0, \tag{2.6c}$$

subject to the boundary conditions

$$f(0) = f'(0) = 0, \quad f'(\infty) = T(\infty) = 1, \tag{2.6d}$$

$$\text{and} \quad T(0) = T_w \quad (\text{fixed wall} - \text{temperature}), \quad \text{or} \quad T'(0) = 0 \quad (\text{insulated wall}). \tag{2.6e}$$

For simplicity we will focus attention on $Pr = 1$, and denote by T_r the wall temperature when the boundary is insulated. Then, as is well known (e.g. Stewartson 1964), the energy equation can be integrated to yield

$$T = 1 + ((T_b - 1) + \frac{1}{2}(\gamma-1)M^2(T_b + f'))(1 - f'), \tag{2.7}$$

where $T_w = T_b T_r$ and $T_r = 1 + \frac{1}{2}(\gamma-1)M^2$.

The solution to (2.6) in the limit of large Mach number has been examined by Freeman & Lam (1959). They showed that two asymptotic regions develop, defined as where the coordinates η and $\xi = M^{\frac{1}{2}}\eta$, respectively, are order one.

$\underline{\xi = O(1)}$

In this region we write $f = M^{-\frac{1}{2}} f_0(\xi) + \ldots$, then using (2.7) it follows from (2.6b) that

$$f_0 f_0'' + \left(\frac{8}{\gamma - 1}\right)^{\frac{1}{2}} \left(\frac{f_0''}{(T_b + f')^{\frac{1}{2}}(1 - f')^{\frac{1}{2}}}\right)' = 0, \tag{2.8a}$$

with

$$f_0(0) = f_0'(0) = 0, \tag{2.8b}$$

and

$$f_0 \sim \xi + \beta + \frac{24}{(T_b + 1)(\gamma - 1)\xi^3} - \frac{72\beta}{(T_b + 1)(\gamma - 1)\xi^4} + \ldots \text{ as } \xi \to \infty. \tag{2.8c}$$

We note that as $\xi \to \infty$, then $f_0' \to 1$ algebraically. This is of course different than the corresponding result for a Chapman fluid, in that case the correction term to the free-stream speed is exponentially small. This difference is significant because it leads to inviscid instabilities which are unstable at very different wavelengths.

$\underline{\eta = O(1)}$

Here, we write

$$f = \eta + \frac{\beta}{M^{\frac{1}{2}}} + \frac{g_1}{M^2} + \cdots, \tag{2.9}$$

then g_1 satisfies the equation

$$\eta g_1'' + 2\left(\frac{\sqrt{1 - \frac{1}{2}(\gamma - 1)(T_b + 1)g_1'}}{1 + C - \frac{1}{2}(\gamma - 1)(T_b + 1)g_1'} g_1''\right)' = 0, \tag{2.10a}$$

subject to

$$g_1 \sim \frac{24}{(T_b + 1)(\gamma - 1)\eta^3} \quad \text{as} \quad \eta \to 0, \quad \text{and} \quad g_1 \to 0 \quad \text{as} \quad \eta \to \infty. \tag{2.10b}$$

In Figure (2.1a) we show the function f_0' for the adiabatic case $T_b = 1$ with $\gamma = 1.4$, we note the algebraic approach of the function to the free-stream speed. In Figure (2.1b) we show the transition layer function g_1' corresponding to the same case. We note the

exponential decay of this function for large η. It is also worth pointing out that for a Chapman fluid the transition-layer equation corresponding to (2.10a) is linear, and it's solution can be expressed in terms of the exponential function. It was this simplification that enabled Smith and Brown (1989) to spot the exact solution of the neutral vorticity mode in their study of the instability problem in this layer. We shall see below that for Sutherland's law we are not able to find a similar exact solution of the stability equation.

Sufficiently far downstream the quasi-parallel assumption is valid for inviscid instability modes. It is then appropriate to seek perturbations of the form

$$u = f'(\eta) + \ldots + \Delta\tilde{u}(\eta)\exp\left(i\sqrt{\frac{R}{(1+C)}}\,(\alpha x + \beta z - ct)\right) + \ldots, \qquad (2.11a)$$

$$p = \frac{1}{\gamma M^2} + \ldots + \Delta\tilde{p}(\eta)\exp\left(i\sqrt{\frac{R}{(1+C)}}\,(\alpha x + \beta z - ct)\right) + \ldots, \qquad (2.11b)$$

with similar expressions for the other flow quantites. If the disturbance amplitude, Δ, is sufficiently small the pressure perturbation $\tilde{p}$ satisfies the compressible Rayleigh equation

$$\frac{d^2\tilde{p}}{d\eta^2} - \frac{2f''}{f'-c}\frac{d\tilde{p}}{d\eta} - (\alpha^2+\beta^2)T(T - \frac{\alpha^2M^2(f'-c)^2}{(\alpha^2+\beta^2)})\tilde{p} = 0, \qquad (2.12a)$$

where for convenience we have rescaled the quantities α, β, c by dividing them by $x^{\frac{1}{2}}$. The conditions that there is no normal velocity at the wall, and that the disturbance is confined to the boundary layer, can be expressed as

$$\tilde{p}' = 0 \text{ on } \eta = 0, \quad \tilde{p} \to 0 \text{ as } \eta \to \infty. \qquad (2.12b)$$

Equation (2.12a) and boundary conditions (2.12b) specify a temporal-stability eigenrelation $c \equiv c(\alpha, \beta)$; alternatively from a spatial stability standpoint, the eigenrelation can be regarded as $\alpha \equiv \alpha(c, \beta)$.

3. THE FAR DOWNSTREAM BEHAVIOUR OF THE INVISCID MODES

In this section we discuss the asymptotic form of unstable solutions to (2.12a) for the region far downstream of the leading edge of the plate. In a previous investigation Cowley and Hall (1988), hereafter referred to as CH, studied the so-called acoustic modes of (2.12a) in this region on the assumption that the viscosity satisfies Chapman's law. Simultaneously Smith and Brown (1989), hereafter referred to as SB, investigated the vorticity mode for Chapman's law. The main difference between these two types of modes is that the acoustic modes have $\alpha \sim M^{-2}$, whilst the vorticity mode, at least while it is close to neutral, has $\alpha \sim \sqrt{2 \log M^2}$. Moreover the vorticity mode is centred at the adjustment layer at the edge of the boundary layer whilst the acoustic one is concentrated in the main part of the boundary layer.

However, as indicated above, at high Mach numbers the temperature variations in the boundary layer are large, so that a *linear* temperature-viscosity law is a bad approximation; Sutherland's law should be used to give a better representation of the viscosity. It is then important to see how the asymptotic structures developed by CH and SB change. We shall see that there are significant differences.

In the first instance we derive the asymptotic structure of the solution for a two-dimensional vorticity mode of (2.12a). We determine the neutral values of α and c for this mode, and find the limiting form of the mode when the further limit $\alpha \to 0$ is taken. This limiting solution points to a sequence of distinguished asymptotic limits. Within the sequence of asymptotic limits mentioned above the scaling, $\alpha \sim M^{-3/2}$, appropriate to an acoustic mode emerges; we therefore discuss the latter mode as a limiting case of the vorticity mode.

$\alpha = O(1)$

Consider then the solution of (2.12a) which has the eigenfunction trapped in the temperature adjustment layer at the edge of the boundary layer. We seek a solution which has $\beta = 0$ and $\alpha = O(1)$, so that the wavelength of the vorticity mode is comparable with the depth of the adjustment layer in terms of the Dorodnitsyn-Howarth variable. From (2.7) and (2.9), the velocity field, $\bar{u}$, and temperature field, $\bar{T}$, of the underlying steady flow expand as

$$\bar{u} = 1 + \frac{2G(\bar{\eta})}{(\gamma - 1)(T_b + 1)M^2} + \ldots, \qquad (3.1a,b)$$
$$\bar{T} = 1 - G + \ldots,$$

where $\eta = \sqrt{2}\bar{\eta}$ and the function $G = \frac{1}{2}(T_b + 1)(\gamma - 1)g_1'$ satisfies a rescaled version of (2.10a), and has the asymptotic behaviour

$$G = -\frac{9}{\bar{\eta}^4} + \frac{B}{\bar{\eta}^{3-\sqrt{7}}} + (2C + 1) + \ldots \quad \text{as} \quad \bar{\eta} \to 0, \tag{3.2a}$$

$$G \to 0 \quad \text{exponentially as} \quad \bar{\eta} \to \infty. \tag{3.2b}$$

Here B is a constant to be calculated numerically.

Next we expand α, c and $\tilde{p}$ in the forms

$$\begin{aligned} \alpha &= \frac{1}{\sqrt{2}}\hat{\alpha} + \ldots, \\ c &= 1 + \frac{2}{(\gamma - 1)(T_b + 1)M^2}\hat{c} + \ldots, \\ \tilde{p} &= \hat{p} + \ldots, \end{aligned} \tag{3.3a, b, c}$$

where we have assumed that the disturbance moves downstream with the fluid speed in the adjustment layer. On substituting for $\bar{u}$ and $\bar{T}$ from (3.1), and using (3.3), we find that the zeroth order approximation to (2.12a) in the adjustment layer is,

$$\frac{d^2\hat{p}}{d\bar{\eta}^2} - \frac{2G'}{G - \hat{c}}\frac{d\hat{p}}{d\bar{\eta}} - \hat{\alpha}^2(1 - G)^2\hat{p} = 0. \tag{3.4}$$

We note that three-dimensional disturbances satisfy (3.4) but with $\hat{\alpha}$ replaced by $\hat{\alpha}^2 + \hat{\beta}^2$ so that in the present regime it is sufficient for us to consider only two-dimensional modes. Equation (3.4) is to be solved subject to $\hat{p}$ vanishing in the limits $\bar{\eta} \to 0$ and $\bar{\eta} \to \infty$, so that the disturbance is confined to the adjustment layer. For $\bar{\eta} >> 1$ it follows from (3.4) that $\hat{p}$ decays like $\exp(-\hat{\alpha}\bar{\eta})$, whilst for $\bar{\eta} << 1$ a WKB solution of (3.4) can be expressed in the form

$$\hat{p} \sim \exp[-\int \Theta(\bar{\eta})]d\bar{\eta}, \tag{3.5}$$

where

$$\Theta \sim -\frac{9\hat{\alpha}}{\bar{\eta}^4} + \frac{2}{\bar{\eta}} + \frac{B\hat{\alpha}}{\bar{\eta}^{3-\sqrt{7}}} + 2C\hat{\alpha} + \ldots \quad \text{as} \quad \bar{\eta} \to 0. \tag{3.6}$$

First, we restrict our attention to the neutral case. $\hat{c}$ is then real and can be evaluated by finding the fluid speed correct to order M^{-2} at the generalized inflection point which is located where

$$\frac{\bar{u}_{\eta\eta}}{\bar{u}_\eta} - \frac{2\bar{T}_\eta}{\bar{T}} = 0,$$

i.e. where

$$\frac{G''}{G'} + \frac{2G'}{1-G} = 0.$$

A numerical solution to (2.10a) using a Runge-Kutta method shows that this occurs when $\bar{\eta} \simeq 1.971510$, in which case

$$\hat{c} = -.993934 \tag{3.7}$$

The corresponding real value of $\hat{\alpha}$ is obtained by integrating (3.4) from $\bar{\eta} = 0$ to $\bar{\eta} = \infty$ with an appropriate treatment at the generalised inflection point. Such a calculation predicts that the neutral value of $\hat{\alpha}$ is

$$\hat{\alpha} \approx 0.645065. \tag{3.8}$$

However, of greater significance are the unstable eigenmodes. Figure (3.1) illustrates the dependence of the growth rate, $\hat{\alpha}\hat{c}_i$, on the real wavenumber $\hat{\alpha}$. We see that the growth rate attains it's maximum value of $\simeq 0.256853$ at $\hat{\alpha} \simeq 0.143619$; further it turns out that the acoustic modes have smaller growth rates (see below) so that this is the most unstable inviscid mode for a hypersonic boundary layer. In Figure (3.2) we show the eigenfunction of the vorticity mode equation at different values of the wavenumber. This figure indicates that as the wavenumber decreases the eigenfunction starts to expand out of the transition layer. We note here that $\hat{c}_i$ as defined above is independent of T_b and that the growth rate is obtained from (3.3b) by dividing $\hat{\alpha}\hat{c}_i$ by $\frac{1}{\sqrt{2}}(T_b + 1)(\gamma - 1)$. It follows that wall cooling has a destabilizing effect on the vorticity mode.

The structure of the growth-rate curves at small wavenumbers is of interest because for sufficiently small values of the wavenumber we expect that the vorticity mode will develop a structure similar to that of the acoustic mode. In the following discussion we will isolate the different significant regimes which occur in the small wavenumber limit. For simplicity we shall now concentrate on the adiabatic problem and take $T_b = 1$.

The key to understanding the subsequent regimes when $\hat{\alpha}$ is related to inverse powers of the Mach number is to write down the small $\hat{\alpha}$ asymptotic structure of (3.4). Figure (3.3) is a schematic illustration of the different regions in $\bar{\eta}$ space which emerge in the limit $\hat{\alpha} \to 0$. Also shown in this figure is the wall layer in which the temperature becomes of order M^2. For the moment $\hat{\alpha}$ is not considered to be sufficiently small for $\hat{\alpha}$ to be $O(M^{-\phi})$ for some positive ϕ; it then turns out that the regions I and IV shown in figure (3.3) are quite passive. However, at sufficiently small values of $\hat{\alpha}$ the wall layer structure of the basic state will enter the problem - see below.

After some careful numerical calculations at small values of $\hat{\alpha}$ we deduced that $\hat{c}$ expands in the form

$$\hat{c} = \frac{\hat{c}_1}{\hat{\alpha}^{4/7}} + \frac{\hat{c}_2}{\hat{\alpha}^{3/7}} + \ldots . \tag{3.9}$$

Also, from (3.2b,4) it follows that for $\bar{\eta} \sim \hat{\alpha}^{-1}$ the pressure decays like $\exp(-\hat{\alpha}\bar{\eta})$. This suggests that the pressure in III should be expanded in the form

$$\begin{aligned} \hat{p} = 1 + \hat{\alpha}^{\frac{1}{7}}\hat{p}_1 + \hat{\alpha}^{\frac{2}{7}}\hat{p}_2 + \ldots + \hat{\alpha}^{\frac{6}{7}}\hat{p}_6 + \hat{\alpha}(\hat{p}_7 - \bar{\eta}) + \\ \hat{\alpha}^{\frac{8}{7}}(\hat{p}_8 - \hat{p}_1\bar{\eta}) + \hat{\alpha}^{\frac{9}{7}}(\hat{p}_9 - \hat{p}_2\bar{\eta}) + \hat{\alpha}^{\frac{10}{7}}(\hat{p}_{10} - \hat{p}_3\bar{\eta}) + \\ + \hat{\alpha}^{\frac{11}{7}}\hat{P}_{11} + \hat{\alpha}^{\frac{12}{7}}\hat{P}_{12} + \hat{\alpha}^{\frac{13}{7}}\hat{P}_{13} + \hat{\alpha}^2\hat{P}_{14} + \ldots , \end{aligned} \tag{3.10}$$

where we have anticipated the form of several terms in this expansion in that $\hat{p}_1, \hat{p}_2, \ldots, \hat{p}_{10}$ are taken as constants, whilst $\hat{P}_{11}, \hat{P}_{12}$, etc. are functions of $\bar{\eta}$. At order $\hat{\alpha}^{\frac{11}{7}}$ in this expansion we find that $\hat{P}_{11}$ satisfies

$$\hat{P}_{11}'' - \frac{2G'}{\hat{c}_1} = 0,$$

so that after use of the exponential mathching condition it follows that

$$\hat{P}_{11} = -\frac{2}{\hat{c}_1}\int_{\bar{\eta}}^{\infty} G d\bar{\eta} - \hat{p}_4\bar{\eta} + \hat{p}_{11}, \tag{3.11}$$

where $\hat{p}_{11}$ is another constant. $\hat{P}_{12}$ and $\hat{P}_{13}$ satisfy similar equations with forcing functions coming from the higher order terms in the expansion of the wavespeed.

The order $\hat{\alpha}^2$ term in (3.10) is then found to satisfy

$$\hat{P}_{14}'' = (1-G)^2 - \frac{2G'}{\hat{c}_1}(\hat{p}_3 - \frac{\hat{c}_2}{\hat{c}_1}\hat{p}_2 - (\frac{\hat{c}_3}{\hat{c}_1} - \frac{\hat{c}_2}{\hat{c}_1})\hat{p}_1 - \frac{\hat{c}_4}{\hat{c}_1} + \frac{2\hat{c}_2\hat{c}_3}{\hat{c}_1^2} - \frac{\hat{c}_2^3}{\hat{c}_1^3}),$$

which may be integrated twice to give $\hat{P}_{14}$. However it is enough for our purposes to note that when $\bar{\eta} \to 0$, $\hat{P}_{14} \sim \bar{\eta}^{-6}$ so that as $\bar{\eta} \to 0$ the order $\hat{\alpha}^{\frac{11}{7}}$ and $\hat{\alpha}^2$ terms in (3.10) become comparable when $\bar{\eta} = O(\hat{\alpha}^{\frac{1}{7}})$; thus, as anticipated earlier, the sublayer III is of depth $\hat{\alpha}^{\frac{1}{7}}$. Within this layer we define

$$Z = \hat{\alpha}^{-\frac{1}{7}}\bar{\eta}$$

and expand the pressure as

$$\hat{p} = 1 + \hat{\alpha}^{\frac{1}{7}}\hat{p}_1 + \ldots + \hat{\alpha}\hat{p}_7 + \hat{\alpha}^{\frac{8}{7}}\tilde{P}_8(Z) + \ldots ,$$

where we have, by matching with the solution in II, again anticipated several terms in this expansion. At order $\hat{\alpha}^{\frac{8}{7}}$ we find that $\tilde{P}_8$ satisfies

$$\tilde{P}_8'' + \frac{72}{Z(\hat{c}_1 Z^4 + 9)}\tilde{P}_8' = \frac{81}{Z^8}.$$

We write the solution for $\tilde{P}_8$ in the form

$$\tilde{P}_8' = (\hat{c}_1 + \frac{9}{Z^4})^2(\int_\infty^Z \frac{81dZ}{(\hat{c}_1 Z^4 + 9)^2} - \frac{1}{\hat{c}_1^2}),$$

where the constant of integration has been chosen to satisfy $\tilde{P}_8' \to -1$ as $Z \to \infty$ in order to match with the solution in II. Finally we consider Region IV and define $\bar{\eta} = \hat{\alpha}^{\frac{1}{3}} z$. The zeroth order approximation to (3.4) here is

$$\hat{p}_{zz} + \frac{8}{z}\hat{p}_z - \frac{81}{z^8}\hat{p} = 0, \tag{3.12}$$

which must be solved subject to $\hat{p} \to 0$ as $z \to 0$. The appropriate solution then has $\hat{p} \to$ constant as $z \to \infty$ so a match with III can only be achieved if

$$\int_0^\infty \frac{81dZ}{(\hat{c}_1 Z^4 + 9)^2} - \frac{1}{\hat{c}_1^2} = 0. \tag{3.13}$$

It is assumed that $\hat{c}_1$ in (3.13) is complex so that after a little manipulation we obtain

$$\hat{c}_1 = -(\frac{8\sqrt{2}}{3\sqrt{3}\pi})^{\frac{4}{7}} \exp(-\frac{3i\pi}{7}),$$

which corresponds to an unstable mode of (2.12a).

$$\underline{\alpha = O(M^{-\frac{3}{2}})}$$

Next we consider the situation when α is so small that IV in Figure (3.3) merges with the wall layer of the basic state. At this stage the wall layer is of thickness $M^{-\frac{1}{2}}$ so that $\alpha \sim M^{-\frac{3}{2}}$. The wavenumber α is then written in the form

$$\alpha = \frac{\alpha_0}{M^{\frac{3}{2}}} + \ldots,$$

where for the moment we shall not be precise about the size of the first correction term in this expansion. The zeroth order approximation to (2.12a) in the wall layer then becomes

$$\tilde{p}'' - \frac{2\bar{u}_0'}{\bar{u}_0 - 1}\tilde{p}' - \frac{\alpha_0^2(\gamma-1)^2}{4}(1+\bar{u}_0)^2(1-\bar{u}_0)^2(1 - \frac{2(1-\bar{u}_0)}{(\gamma-1)(1+\bar{u}_0)})\tilde{p} = 0, \tag{3.14}$$

where a dash denotes a derivative with respect to the wall layer variable $\xi = M^{\frac{1}{2}}\eta$, and $\bar{u}_0$ is the first term in the expansion of $\bar{u}$ in that layer. The above equation is again to be solved subject to $\tilde{p}'(0) = 0$. For large ξ it has the asymptotic solutions

$$\tilde{p} \sim N_0 = \text{constant} \quad \text{and} \quad \tilde{p}\xi^7 \sim N_1 = \text{constant}.$$

For most values of α_0 the constant N_0 is nonzero, and the structure in layers I, II, III survives intact. Thus for these values of α_0 the wavespeed c expands as

$$c = 1 - \frac{d_1}{M^{\frac{8}{7}}} + \ldots, \tag{3.15}$$

and d_1 will be complex so that the wave growth rate is of order $M^{-\frac{37}{14}}$.

However, equation (3.14) has a countable infinite set of eigenvalues for which the constant $N_0 = 0$. In this case the eigenfunction takes on its greatest value in the wall layer, i.e. where the steady velocity field is adjusting to it's free-stream value. These eigenvalues correspond to the acoustic inviscid modes and are the counterpart of those discussed by CH. A numerical solution of (3.14) yielded the sequence $\alpha_0 = 2.47$, 7.17, 12.19, 17.33, 22.54, 27.79, ... The first three eigenfunctions associated with this sequence of eigenfunctions are shown in Figure (3.4). Thus at a countable discrete set of points the acoustic modes emerge as almost neutral "vorticity" modes. In fact we could seek acoustic modes with $\alpha \sim O(1)$, i.e. for a wavenumber much larger than currently assumed, for which the eigenfunction is concentrated in the $\xi = O(1)$ wall layer. These modes have a fast variation in this layer which may be described by the WKB method. At certain values of M these eigenvalues coalesce with the neutral vorticity mode discussed earlier, and an analysis outlined in CH (see also SB) can be performed to describe the 'splitting' of the eigenvalues in this region, we do not pursue that calculation here but simply determine the structure of the vorticity mode in the vicinity of the acoustic mode. Thus the small α structure outlined above remains valid for $\alpha = O(M^{-\frac{3}{2}})$ if the acoustic modes are avoided; it follows that c_i continues to grow in the further limit $\alpha M^{\frac{3}{2}} \to 0$, where no neutral acoustic modes exist.

In order to examine the interaction of the vorticity mode with the acoustic modes in a little more detail, we expand the wavenumber in the form

$$\alpha = \frac{\alpha_0^*}{M^{3/2}} + \frac{\alpha_1^*}{M^{25/14}} + \ldots,$$

whilst c still expands as in (3.15). Here we are denoting by α_0^* any eigenvalue of (3.14) corresponding to $N_0 = 0$. In the wall layer $\tilde{p}$ expands as

$$\tilde{p} = M^{2/7} Q_0 (1 + \Phi[M]) + Q_1 + \dots, \tag{3.16}$$

where we have anticipated the possible occurrence of further eigenfunctions between Q_0, Q_1 by inserting the factor $(1 + \Phi[M])$. For our purposes it is not necessary for us to calculate Φ here. If we substitute the above expansion into Rayleigh's equation we see that Q_0 satisfies (3.14) with $\alpha = \alpha_0^*$. The derivative of Q_0 vanishes at $\xi = 0$ whilst for $\xi >> 1$

$$Q_0 \sim q_0 \xi^{-7}$$

where q_0 is a constant. At higher order in Rayleigh's equation we find that Q_1 satisfies

$$Q_1'' - \frac{2\bar{u}_0'}{\bar{u}_0 - 1} Q_1' - \frac{(\alpha_0^*)^2(\gamma-1)^2}{4}(1-\bar{u}_0^2)(1 - \frac{2(1-\bar{u}_0)}{(\gamma-1)(1+\bar{u}_0)})Q_1$$
$$= \frac{\alpha_1^* \alpha_0^*}{2}(\gamma-1)^2(1-\bar{u}_0^2)(1 - \frac{2(1-\bar{u}_0)}{(\gamma-1)(1+\bar{u}_0)})Q_0.$$

The solution of this equation which has $Q_1'(0) = 0$ is such that for large ξ

$$Q_1 \sim a_0 q_0 \alpha_1^*.$$

The constant a_0 depends on α_0^* and γ, and can only be determined numerically. However it can be shown that a_0 is alternatively positive and negative at successive values of α_0^*. The region III of Figure (3.3) becomes of depth $O(M^{-3/14})$ when α is $O(M^{-3/2})$. The solution in this layer is calculated using the procedure outlined above; the only significant change is that in matching regions III and IV we must now account for the fact that $Q_0 \sim \xi^{-7}$ for large ξ. After some manipulation we find that the eigenrelation obtained when this matching has been carried out is

$$\frac{1}{\tilde{\alpha}_1^*} = \frac{1}{\tilde{d}_1^2} + \frac{1}{\tilde{d}_1^{1/4} e^{i\pi/4}}, \tag{3.17}$$

where

$$\tilde{\alpha}_1^* = \frac{9A^2 a_0 \alpha_0^* \alpha_1^*}{7D^2}, \quad \tilde{d}_1 = D d_1, \quad D = (9\frac{\alpha_0^*}{8\sqrt{2}})^{4/7}, \quad A = \frac{12}{(\gamma-1)}. \tag{3.18a,b,c,d}$$

In Figure (3.5) we have shown solutions of (3.17) for $-5 < \tilde{\alpha}_1^* < 5$. At both ends of this Figure $\tilde{d}_1$ approaches $e^{-\frac{3i\pi}{7}}$ which gives the required matching with the unstable vorticity

modes away from the acoustic modes. We further note that for small α_1^* the growth rate tends to zero. More precisely from (3.17) we find that for small α_1^*

$$\bar{d}_1 \sim (\tilde{\alpha}_1^*)^{1/2} + \frac{\tilde{\alpha}_1^{*\,1/8} e^{-i\pi/4}}{2} + \ldots$$

so that, dependent on on the sign of α_1^*, the growth rate goes to zero like $M^{-\frac{3}{2}}(\tilde{\alpha}_1^*)^{1/2}$ or $M^{-\frac{3}{2}}(\tilde{\alpha}_1^*)^{11/8}$.

Strictly we should now rescale the above expansions when α_1^* becomes sufficiently small. We do not pursue that rescaled problem here since our main concern is with completing a discussion of the structure of the vorticity mode at all lengthscales, in particular we wish to see if the vorticity mode connects with any other neutral states. We have already seen that c_i continues increasing as the wavenumber decreases through $O(M^{-3/2})$ values, apart from small neighborhoods of the acoustic modes where it decrease towards zero. Thus c_i tends to infinity on the present scaling when α_0 tends to zero. Thus the main significance of the $\alpha \sim M^{-3/2}$ regime is that it is at this stage where the acoustic modes emerge; however the small α structure, developed initially for the $\alpha = O(1)$ scaling, survives this regime intact in the limit of α_0 tending to zero.

$$\underline{\alpha = O(M^{-\frac{7}{4}})}$$

The next significant stage in the development of the vorticity mode occurs when the temperature in the upper layer, i.e. where $\eta \sim \alpha^{-1}$, becomes such that $\bar{T} \sim (\bar{u} - c)^2 M^2$. The pressure eigenfunction in the upper layer then has its decay to zero modified. This situation occurs when

$$c = 1 - \frac{\bar{d}_1}{M} + \ldots, \tag{3.18}$$

with

$$\alpha = \frac{l}{M^{7/4}} + \ldots. \tag{3.19}$$

In this case the pressure in the upper layer decays like $\exp(-l(1-\bar{d}_1^2)^{\frac{1}{2}} M^{-7/4}\eta)$. This means that in the rescaled region corresponding to III of Figure (3.2), where we write $Z = M^{1/4}\eta$, the pressure perturbation expands as

$$\tilde{p} = 1 + \ldots + \frac{\tilde{P}_2(Z)}{M^2} + \ldots.$$

and $\tilde{P}_2$ satisfies the equation

$$\tilde{P}_2'' - \frac{24A}{Z[\bar{d}_1 Z^4 - 3A]}\tilde{P}_2' = \frac{9A^2(\gamma-1)^2 l^2}{Z^8}.$$

The solution of this equation which enables us to match with the behaviour discussed above is

$$\tilde{P}_2' = (\bar{d}_1 - \frac{3A}{Z^4})(-\int_z^\infty \frac{9A^2(\gamma-1)^2 l^2}{(\bar{d}_1 Z^4 - 3A)^2} dZ - l\sqrt{\frac{1-\bar{d}_1^2}{\bar{d}_1^2}}).$$

In the wall layer there are now no acoustic mode eigenfunctions which lead to decay at infinity so that matching leads to the eigenrelation

$$\int_0^\infty \frac{9A^2(\gamma-1)^2}{(\bar{d}_1 Z^4 - 3A)^2} dZ + \frac{l\sqrt{1-\bar{d}_1^2}}{\bar{d}_1^2} = 0.$$

A more convenient form for the eigenrelation is found by writing

$$l = \frac{8\bar{l}\sqrt{2}}{3(3A)^{1/4}(\gamma-1)^2\pi}$$

so that

$$\bar{\ell} e^{-i\pi/4} + \bar{d}_1^{\frac{7}{4}}\sqrt{1-\bar{d}_1^2} = 0.$$

As expected in the limit $\bar{\ell} \to \infty$ we obtain $\bar{d}_1 \sim e^{-3i\pi/7}\bar{\ell}^{-\frac{4}{7}}$ which is the limiting form of the solution obtained for $\alpha \sim M^{-\frac{3}{2}}$. It is a simple matter to show from the above equation that $\bar{d}_{1i}$ is a monotonic decreasing function of $\bar{\ell}$ and in particular for $\bar{\ell} \to 0$ we find that

$$\bar{d}_1 \sim \bar{\ell}^{-\frac{4}{3}} e^{-i\pi/3}. \tag{3.20}$$

The main implication of this limit is that the $M^{-\frac{1}{4}}$ layer for the $\alpha \sim M^{-\frac{7}{4}}$ modes decreases in size like $\bar{\alpha}_1^{-\frac{7}{4}}$ when $\bar{\ell}_1 \to 0$. The next stage is when the $M^{-\frac{1}{4}}$ and $M^{-\frac{1}{2}}$ layers merge which occurs when $\bar{d}_1 = O(M)$ and $\alpha = O(M^{-\frac{5}{2}})$.

$$\underline{\alpha = O(M^{-\frac{5}{2}})}$$

Here we expand c and α in the forms

$$c = c_0 + \ldots, \quad \alpha = \frac{L}{M^{\frac{5}{2}}} + \ldots.$$

Now there are just three regions, of depth $M^{-\frac{1}{2}}, M^0$, and $M^{\frac{3}{2}}$, for us to consider. Interestingly the extent of the perturbation away from the wall has been reduced by a factor of $M^{\frac{1}{4}}$ from the order $M^{\frac{7}{4}}$ scale of the case $\alpha \sim M^{-\frac{3}{2}}$. This reduction in depth is caused by $(\bar{u} - c)$ remaining $O(1)$ in this layer, and if we write $\eta = M^{\frac{3}{2}}Y$, the dominant terms in the equation for the pressure in that layer give

$$\tilde{p}_{YY} + L^2(1-c_0)^2\tilde{p} = 0 \tag{3.21}$$

If c_0 has a positive imaginary part, it follows that

$$\tilde{p} = \exp(-\sigma Y),$$

with $\sigma = iL(1 - c_0)$. Thus where $Y \to 0$ we have that $\frac{d\tilde{p}}{d\eta} \to -M^{-\frac{1}{2}}\sigma$. This means that the required solution for $\tilde{p}$ in the $\eta = O(1)$ region is

$$\tilde{p} = 1 + \ldots - \frac{\sigma}{M^{\frac{1}{2}}}[p_{\frac{1}{2}} + \eta] + \ldots. \tag{3.22}$$

Here the constant terms are small compared to M^0 but large compared to $M^{-\frac{1}{2}}$; in principle they may be found by matching requirements. It remains to consider the small layer when $\eta = M^{-\frac{1}{2}}\xi$, and $\tilde{p}$ expands as

$$\tilde{p} = 1 + \ldots + \frac{1}{M^2}\bar{P}_2(\xi) + \ldots.$$

$\bar{P}_2$ is found to satisfy

$$\bar{P}_2'' - \frac{2u_0'}{u_0 - c_0}\bar{P}_2' = \frac{1}{2}L^2(\gamma - 1)(1 + u_0)(1 - u_0)(\frac{1}{2}(\gamma - 1)(1 + u_0)(1 - u_0) - (u_0 - c)^2)$$

so that

$$\bar{P}_2' = (u_0 - c_0)^2 \int_0^\xi \frac{L^2(\gamma - 1)(1 + u_0)(1 - u_0)}{2(u_0 - c_0)^2}(\frac{(\gamma - 1)(1 + u_0)(1 - u_0)}{2} - (u_0 - c_0)^2)d\xi. \tag{3.22}$$

A match with the core solution is achieved if

$$(1 - c_0)^2 \int_0^\infty \frac{L^2(\gamma - 1)(1 + u_0)(1 - u_0)}{4(u_0 - c_0)^2}((\gamma - 1)(1 + u_0)(1 - u_0) - 2(u_0 - c_0)^2)d\xi$$
$$= -\sigma = -iL(1 - c_0). \tag{3.23}$$

This is the required eigenrelation to determine the complex wavespeed c_0 as a function of the scaled wavenumber L. A large L analysis of this equation shows that the limiting small $\bar{\ell}$ solution of the $\alpha = O(M^{-\frac{1}{2}})$ case is retrieved.

In Figure (3.6) we show c_0 as a function of L for $100 < L < 400$ and the case of an insulated wall. We see that the maximum value of c_i for a two-dimensional mode occurs for $L \sim 225$ and a neutral mode exists for $L \sim 110$. We postpone until the final section a discussion of the implications of the results we have found above.

4 The Inviscid Instability Problem in Interactive Boundary Layers.

We consider the hypersonic flow of a Sutherland law fluid past the semi infinite wall defined by the positive x axis. The oncoming flow has constant velocity at infinity and the leading edge of the wall is sharp. This results in the formation of a shock wave which acts as an upper bound for the flow disturbances in the sub-layers below, the uppermost of which is inviscid. The reader is referred to Figure (4.1) for a description of the different parts of the flow field.

This region has been studied by for example, Bush (1966), and since viscosity is negligible here the use of a power-viscosity-temperature law does not alter the well-known governing equations for this region. Below the expansions and equations governing the flow are given. Apart from some minor differences, our formulation is essentially the same as that of, amongst others, Stewartson (1955, 1964) and Bush (1966) and so the reader is referred to those papers for more details.

The flow quantities and coordinates have been non-dimensionalised using upstream flow quantities and L a typical streamwise lengthscale. We then scale the non-dimensionalised normal coordinate y appropriately

$$y = \frac{Y}{M}, \tag{4.1}$$

where M is the Mach Number and Y is taken to be $O(1)$. Note that as yet we do not scale the downstream variable x. As in previous studies we consider the two-dimensional problem and this enables the introduction of a streamfunction ψ defined by

$$\rho u = \psi_y \ , \qquad \rho v = -\psi_x \tag{4.2a,b}$$

Further we expand the velocity, temperature, density, pressure and streamfunction as

$$u = 1 + \frac{u_1}{M^2} + \cdots \ , \qquad v = \frac{v_1}{M} + \cdots,$$

$$T = T_1 + \cdots \ , \qquad \rho = \rho_1 + \cdots \ , \qquad p = \frac{p_1}{M^2} + \cdots, \tag{4.3a,b,c,d,e,f}$$

and

$$\psi = \frac{1}{M}\psi_1 + \cdots \ .$$

If the above expansions are substituted into the inviscid Navier-Stokes equations written in Von-Mises coordinates we obtain, after some manipulation, the governing equations for this layer

$$v_{1x} = -p_{1\psi_1} \ , \qquad v_{1\psi_1} = \frac{\partial}{\partial x}\left(\frac{1}{\rho_1}\right) \ , \qquad p_1 = E(\psi_1)\rho_1^{\gamma}. \qquad (4a,b,c)$$

The function $E(\psi_1)$ is evaluated from the initial conditions which for these hyperbolic equations are given at the shock. Conventionally, we define the shock by $Y = f(x)$ where f is unknown at present; we note that $\psi_1 = f$ on the shock.

The Strong Interaction Zone

The solution of these equations (and the corresponding ones for the lower layers) can be investigated analytically in the large $x-$ and small $x-$limits using expansion procedures, following Stewartson (1955, 1964), Brown and Stewartson (1975). The formulation below follows the latter paper closely.

Let us consider the solution of (4.4a,b,c) for small x, i.e. close to the leading edge of the plate, where the shock is attached. Here we write

$$f = a_1 x^{3/4} + \cdots \ , \qquad p_1 = a_1^2 \overline{p}_1(\zeta) x^{-1/2} + \cdots \ ,$$

$$v_1 = a_1 \overline{v}_1(\zeta) x^{-1/4} + \cdots \qquad \text{and} \qquad \rho_1 = \overline{\rho}_1(\zeta) + \cdots \ . \qquad (4.5a,b,c,d)$$

The similarity variable ζ introduced in the above equations is defined by

$$\zeta = \frac{\psi_1}{a_1 x^{3/4}}. \qquad (4.6)$$

The scalings (4.5b,c,d) are implied by the Rankine-Hugoniot relations, which relate flow quantities either side of the shock $Y = f(x)$, and by (4.5a) which follows from matching normal velocities and pressure across the sub-layers beneath the shock; see Stewartson (1964) and references therein.

The resulting equations for the leading order terms are

$$\overline{p}_1(\zeta) = \frac{e_1}{\zeta^{2/3}} \overline{\rho}_1^{\gamma}(\zeta) \ , \qquad \overline{v}_1 + 3\zeta \overline{v}_1' = 4\overline{p}_1',$$

$$\overline{v}_1' = \frac{3\zeta}{4\overline{\rho}_1^2} \overline{\rho}_1' \qquad \text{and} \qquad e_1 = \frac{9(\gamma-1)^{\gamma}}{8(\gamma+1)^{\gamma+1}}, \qquad (4.7a,b,c,d)$$

with

$$\overline{v}_1 = \frac{3}{2(\gamma+1)} \ , \quad \overline{p}_1 = \frac{9}{8(\gamma+1)} \ , \quad \overline{\rho}_1 = \frac{\gamma+1}{\gamma-1} \quad \text{on} \quad \zeta = 1 \ ,$$

which are the conditions at the shock. We require their solution for $\zeta < 1$. In particular, for given γ we can solve numerically for $\overline{v}_1(0)$ and $\overline{p}_1(0)$.

Substitution of (4.5b,d) into (4c) and recalling the definition of ζ gives $E(\psi_1) \sim \rho_1 a_1^{8/3} \psi_1^{-2/3}$ as $\psi_1 \to 0$. This implies that, as $\zeta \to 0$, $\overline{p}_1 \sim \zeta^{2/3\gamma}$ and this produces a higher order correction in $\overline{v}_1$ if $\gamma > \frac{2}{3}$. For a realistic gas γ is larger than this value, with the result that there must be a viscous sublayer beneath the present layer. Bush (1966) found that this layer enables one to match the inviscid-layer solution on to the boundary layer solution if one used a power-viscosity/temperature law ($\mu \sim T^{\omega}, \omega < 1$), rather than the linear law used by Stewartson and most other research studies in the field. Stewartson (1955) hoped that by using idealized assumed physical properties it would help to "understand the behaviour of more realistic fluids". His assumption resulted in discontinuous derivatives, or "kinks", in properties between the Inviscid Zone and the Boundary Layer, see Fig. 7.4, page 167 of Stewartson (1964). Despite the results of Bush (1966) (and a few subsequent authors) the linear viscosity law is still extensively used in hypersonic shock/boundary-layer research; it is argued that these 'kinks' are only a slight nuisance that can probably be explained away by deeper analysis and appeal to the argument of Stewartson concerning the assumption of ideal fluid properties. The analysis of Bush was extended to the linear case by Lee and Cheng (1969). They found that, by consideration of a second order boundary-layer correction, coupled to Bush's transitional layer analysis, the two layer structure of Stewartson gives the correct basis for the flow structure.

Not surprisingly the extensive use of Chapman's law in hypersonic calculations has encouraged researchers in stability theory to make the same rather severe approximation to the fluid viscosity; we believe that the calculations given in this paper are the first to take account of a realistic viscosity-temperature dependence in a first mode stability analysis. We note that our flow solutions in the layers beneath the shock are in full agreement with Bush, but he considered a general power law whereas we concentrate on $\mu \sim T^{1/2}$, the leading order form for Sutherland's law at high temperatures. For convenience we will use the notation of Stewartson and Brown (1975). We will next consider the viscous-adjustment-layer after discussing the third sub-layer, the viscous boundary layer.

Viscous Boundary Layer

This is adjacent to the surface of the plate and enables velocities to be reduced to zero on the surface. First, the full asymptotic formulation is described briefly, then the

asymptotic behaviour for small x is discussed in the next subsection. We assume that the boundary layer exists where $\psi \sim M^{-3}$, ψ being the stream-function defined earlier. We define the hypersonic parameter r by

$$Re = rM^5 \tag{4.8}$$

and take r to be order one. Note that the power of the Mach number is six in the definitions of the hypersonic parameters of those using a linear viscosity law. We write

$$u = U_1 + \cdots , \qquad v = \frac{V_1}{M} + \cdots , \qquad p = \frac{1}{M^2} P_1 ,$$

$$\rho = \frac{1}{M^2} R_1 + \cdots , \qquad T = M^2 \theta_1 \qquad \text{and} \qquad \mu = M\mu_1. \tag{4.9a,b,c,d,e,f}$$

These scalings are standard apart from that for the viscosity μ which follows immediately from the high temperature form of Sutherland's law:

$$\mu = (1 + C)T^{1/2}. \tag{4.10}$$

We make the assumptions that the Prandtl number is unity and that the wall is insulating, this enables us to carry out a relatively simple analysis for the viscous solutions. The solutions capture the new structure of the inviscid modes due to the effect of using a power-viscosity law in the viscous sublayers. The relaxation of these assumptions does not substantially alter the conclusions obtained below.

We again transfer to von Mises coordinates; using the streamfunction Ψ as an independent variable instead of Y. The energy and momentum equations are combined to yield the boundary-layer equations in these coordinates

$$U_1 U_{1x} = -\frac{(\gamma - 1)}{2} \frac{(1 - U_1^2)}{\gamma P_1} P_{1x} + \frac{\gamma P_1 U_1}{r} \left(\frac{\mu_1}{\theta_1} U_1 U_{1\Psi} \right)_{\Psi},$$

and

$$\theta_1 = \frac{\gamma - 1}{2}(1 - U_1^2), \tag{4.11a,b}$$

together with $\mu_1 = \theta_1^{1/2}$ from (4.10), and with usual boundary conditions

$$U_1 = 0 \quad \text{on} \quad \Psi = 0,$$

$$U_1 \to 1 \quad \text{as} \quad \Psi \to \infty. \tag{4.12a,b}$$

Boundary-Layer Solution for the Strong Interaction Zone

Now let x be small so that the hypersonic interaction parameter becomes large. We define the similarity variable ϕ by

$$\Psi = [4\gamma(1+C)\overline{p}_1(0)]^{1/2}\Big(\frac{2}{\gamma-1}\Big)^{1/4}\frac{a_1 x^{1/4}}{r^{1/2}}\phi, \tag{4.13}$$

where a_1 and $\overline{p}_1(0)$ were introduced when considering the inviscid region. If we now write

$$U_1 = g(\phi) + \cdots, \tag{4.14}$$

we obtain the similarity equation for the boundary-layer solution

$$-\phi g g' = \Big(\frac{\gamma-1}{\gamma}\Big)(1-g^2) + g\Big(\frac{gg'}{(1-g^2)^{1/2}}\Big)'$$

and

$$g(0) = 0\ , \qquad g(\infty) = 1\ . \tag{4.15a,b,c}$$

This is a modified Faulkner-Skan equation, but the decay of g at large ϕ is now algebraic rather than the usual exponential behaviour,

$$g \sim 1 - \frac{\alpha}{\phi^4} + \cdots\ , \qquad \text{as} \qquad \phi \to \infty, \tag{4.16}$$

and $\alpha > 0$ can be determined analytically.

Matching normal velocities across the sub-layers in the usual manner yields the leading order coefficient a_1 in the small x expansion for the as yet unknown shock location

$$a_1^2 = \frac{3(1+C)}{4\overline{v}_1(0)}\Big(\frac{2(\gamma-1)}{r\gamma\overline{p}_1(0)}\Big)^{1/2}\Big(\frac{\gamma-1}{2}\Big)^{1/4}\int_0^\infty \frac{1-g^2}{g}d\phi. \tag{4.17}$$

The Viscous Transition Layer

Here the velocities and temperatures in the outer inviscid flow match with those in the inner boundary-layer flow. We give a brief account of the arguments used to deduce the position and properties of this region and again consider the strong interaction zone.

Earlier it was noted that the inviscid density function $\overline{p}_1 \sim \zeta^{2/3\gamma}$ as $\zeta \to 0$. It can easily be deduced that u_1 and T_1 grow like inverse powers of ζ as $\zeta \to 0$. In fact

$$T \sim T_1 \sim x^{-1/2}\zeta^{-2/3\gamma} \sim x^{-1/2}\Big(\frac{x^{3/4}}{\psi_1}\Big)^{2/3\gamma}\ , \tag{4.18}$$

as $\psi_1 \to 0$.

Now let us consider the boundary-layer temperature as the top of the layer is approached. We have written $T = M^2\theta_1$ and found that $\theta_1 = \frac{\gamma-1}{2}(1 - U_1^2)$. We know the large ϕ behaviour of U_1 and it follows immediately that

$$\theta_1 \sim \frac{1}{\phi^4} \sim \frac{x}{\Psi^4} \sim \frac{x}{m^8\psi_1^4},$$

so that

$$T = m^2\theta_1 \sim \frac{x}{\psi_1^4 m^6} \qquad \text{as} \qquad \phi \to \infty. \tag{4.19}$$

Matching the limiting temperatures (4.18) (4.19) gives the position of the viscous transition layer,

$$\psi_1 \sim M^{-\lambda} x^{(3-\lambda)/4}, \qquad \lambda = \frac{9\gamma}{6\gamma - 1} \tag{4.20a,b}$$

This is in full agreement with Bush's result. Note that the powers involved in the asymptotics are functions of γ, the ratio of specific heat capacities, in the new layer. Further investigation of the small ψ_1 limit of the inviscid solutions implies the following expansions for flow properties in the transition layer

$$\begin{aligned} u &= 1 + M^{\frac{4(2-3\gamma)}{6\gamma-1}} u_1 + \cdots, \\ T &= M^{\frac{6}{6\gamma-1}} T_1 + \cdots, \end{aligned} \tag{4.21a,b,c}$$

together with

$$\rho = \frac{\gamma p_1}{T}.$$

We define the scaled streamfunction η

$$\psi_1 = \eta M^{-\lambda} \quad (= M\psi). \tag{4.22}$$

These are then substituted into the Parabolised Navier-Stokes equations in Von- Mises co-ordinates to obtain the equations for u_1

$$\frac{u_{1x}}{(1+C)} = -\frac{T_1 p_{1x}}{\gamma p_1} + \frac{\gamma p_1}{r}\frac{\partial}{\partial \eta}\left(\frac{1}{T_1^{\frac{1}{2}}}\frac{\partial u_1}{\partial \eta}\right), \tag{4.23}$$

where, as we are taking the Prandtl number to be unity and the wall to be insulating, the corresponding energy equation can be integrated to yield

$$T_1 = (1-\gamma)u_1. \tag{4.24}$$

The pressure p_1 is independent of the normal co-ordinates, as usual in viscous regions governed by the boundary-layer equations, so the pressure is expanded

$$p_1 = \frac{a_1^2 \bar{p}_1(0)}{x^{\frac{1}{2}}} + \cdots$$

in the two viscous layers, this being the limiting form as the inviscid layer is descended.

We see that (from (4.23)) in this adjustment layer we still have the high temperature form of Sutherland's law, in contrast with the shock-free adjustment layer of section 2 where the full form is needed. Again, a similarity solution for the flow exists in this viscous sub-layer with similarity variable z defined by

$$\eta = \beta x^{\Lambda} z, \tag{4.25a}$$

where

$$\beta^2 = \frac{(C+1)\gamma a_1^2 \bar{p}_1(0)}{r}$$

and

$$\Lambda = \frac{3-\lambda}{4}. \tag{4.25b,c}$$

Writing $u_1 = x^{\lambda-2} G(z)$ leads to the governing equation for the flow solution in this crucial region

$$(\lambda-2)G - \frac{(3-\lambda)}{4} z G' = \frac{1-\gamma}{2\gamma} G + \left[\frac{G'}{\sqrt{(1-\gamma)G}} \right]'. \tag{4.26}$$

Note that from the definition of u_1, (4.21a), we expect that $G < 0$. We require that this solution for u_1 matches to the corresponding solutions above and below, i.e. in the inviscid sub-layer and viscous boundary layer respectively, so we must investigate asymptotically the small and large z limiting forms of G.

As $z \to 0$ we find that G has the behaviour

$$G = -g_0 z^{-4} + g_1 z^{-\nu} + \cdots, \quad g_0 = \frac{576\gamma^2}{(\gamma-1)(3\gamma-1)^2}. \tag{4.27a,b}$$

Thus the transition layer solution matches onto the large ϕ form of g. The exponent ν of z in the first correction term can be calculated analytically whilst the coefficient g_1 must be determined from a numerical solution. In fact ν satisfies a quadratic equation with coefficients functions of γ. With $\gamma = 1.4$ we find that $\nu = 0.6267\ldots$ so that we have relatively small correction terms. The value of g_0 for this choice of gamma is 275.6 ... and so G grows quickly as $x \to 0$.

We now investigate the behaviour of G for large z we find that

$$G \to -A_0 z^{-\frac{2}{3\gamma}} + A_1 z^{-2-\frac{1}{3\gamma}} + \cdots, \tag{4.28}$$

and so again we have a relatively small correction term. Note that G decays algebraically, in contrast to the rapid exponential decay of the Blasius and the "Modified Blasius" functions which arise in the shock-free, far-downstream cases (the former after employing the linear Chapman viscosity law and the latter from the use of the more realistic Sutherland's law - see earlier). The second coefficient A_1 is a function of gamma and can be determined in terms of A_0; in fact

$$A_1 = \frac{8A_0^{\frac{1}{2}}(3\gamma+1)}{9\gamma(\gamma-1)^{\frac{1}{2}}(3\gamma-1)}.$$

The constant A_0 is not fixed by the asymptotics. Instead we must choose it so that the velocity solution matches with the appropriate limiting form of the inviscid solution. We obtain, after an elementary matching argument, and a little manipulation, the result

$$A_0 = (1+C)^{-\frac{1}{3\gamma}} \frac{\gamma^{1-\frac{1}{3\gamma}} a_1^2 r^{\frac{1}{3\gamma}} p_{10}^{1-\frac{4}{3\gamma}} e_1^{\frac{1}{\gamma}}}{\gamma-1}. \tag{4.29}$$

For the value $\gamma = 1.4$ we find $A_0 = 0.1751....$ In our numerical calculations we took without loss of generality the hypersonic interaction parameter to be unity. Now that the base flow for this region has been found (at leading order) we can consider its stability characteristics; in particular we are interested here in the linear stability of inviscid modes concentrated (trapped) within this adjustment layer. These so-called vorticity-modes have been discussed earlier for other flows.

The Vorticity Mode in the Strong Interaction Zone

The scalings for these modes appear complicated but follow in a straight-forward manner after applying the usual vorticity mode arguments to the flow field discussed above. The modes of wavenumber k have wavelength comparable with the thickness of the transition region and a Rayleigh analysis suggests we require $\partial_{\psi\psi} \sim T^2 k^2$. This can be seen, for example, from (2.12a) and (3.4) studied earlier. From (4.21b), and recalling the definition of λ in (4.20b), we have $T \sim M^{4\lambda-6}$, and also from (4.22), $\psi \sim M^{-\lambda-1}$. Note that with these scaling we are primarily concerned with obtaining the correct Mach number dependence; the small x dependence will be incorporated later. We deduce that

$k \sim M^{7-3\lambda} >> 1$, and thus this represents a short wavelength mode and so we introduce a fast x-scale

$$X = M^{7-3\lambda} x. \tag{4.30}$$

The time-scale can also be similarly deduced from Rayleigh analysis, after noting that the vorticity modes propagate in a frame moving with uniform velocity and recalling the u_1 scaling (4.21a) . We are lead to the introduction of a short time scale.

$$\tau = M^{\lambda-1} t. \tag{4.31}$$

We note that these scales are compatible with our earlier analysis of the non-interactive case. At leading order we have the multiple-scales

$$\partial_x \rightarrow \partial_x + M^{7-3\lambda}\partial_X \quad , \quad \partial_t \rightarrow M^{\lambda-1}\partial_\tau - M^{7-3\lambda}\partial_X .$$

Note that non-parallel effects are $O(\partial_x) \sim O(1)$ and are negligible in comparison with the direct growth effects of order $k(u-1) = O(M^{\lambda-1}) >> 1$; for our choice of $\gamma = 1.4$ we find that $\lambda = 1.7027$. The wavespeed $\hat{c}$ of the vorticity mode propagating in the frame moving with uniform (nondimensionalised) velocity $u = 1$ is related to its stationary-frame wavespeed c by

$$c = 1 + \frac{\hat{c}}{M^{4(2-\lambda)}} + \cdots \tag{4.32}$$

which follows immediately from (4.21a). Note that it represents a small perturbation about the velocity of the propagating frame. The remainder of the analysis follows the classical inviscid mode approach for formulating the pressure equation for the linear wave-like disturbance, now that the scales have been deduced. We assume that the flow previously discussed for this region is perturbed by an infinitesimal disturbance proportional to

$$e^{ik(X-\hat{c}\tau)} \tag{4.33}$$

containing all the X and τ dependence of the disturbance. We note that the basic flow properties are independent of τ and X allowing such an assumption. After a little manipulation we will obtain the so-called vorticity-made-Rayleigh equation for the amplitude of the disturbance pressure p_η

$$\hat{p}_{\eta\eta} - \frac{2u_{1\eta}}{u_1 - \hat{c}}\hat{p}_\eta - \frac{(\gamma-1)^2 u_1^2}{\gamma^2 p_1^2} k^2 \hat{p} = 0, \tag{4.34}$$

where we require $\hat{p}$ to decay to zero for large and small η. We now return to the Strong Interaction Zone and investigate the asymptotic behaviour of (4.34) for small x.

We recall the leading order small x forms

$$p_1 = \frac{a_1^2 \bar{p}_1(0)}{x^{\frac{1}{2}}}, \quad \eta = \beta x^{\frac{1}{4}(3-\lambda)} z, \qquad (4.35a,b,c)$$
$$u_1 = x^{\lambda-2} G.$$

We need the small-x dependence of $\hat{c}$ and k but need not worry about $\hat{p}$ as (4.34) is linear. We find that

$$\hat{c} = x^{\lambda-2} \mathcal{C},$$

and

$$k = \frac{r\beta}{(\gamma-1)x^{3(\lambda-1)/4}} \mathcal{K}, \qquad (4.36a,b)$$

are the necessary behaviours. The former follows immediately from (4.35c) and the latter results from considering the coefficient of $\hat{p}$ in (4.34). We finally arrive at the renormalised problem for $\hat{p}$; the vorticity-mode pressure-amplitude equation for the strong-interaction zone

$$\hat{p}_{zz} - \frac{2G'}{G-\mathcal{C}} \hat{p}_z - \mathcal{K}^2 G^2 \hat{p} = 0, \qquad (4.37)$$

to be solved subject to $\hat{p}$ vanishing in the limits $z \to 0$ and $z \to \infty$, so that, as in previous analyses, the disturbance is confined to the adjustment layer. We discuss our numerical solution of this eigenvalue problem and its limiting small wavenumber form in the next section.

5 The Solution of the Strong Interaction Vorticity Mode Equation.

The leading order asymptotes of equation (4.37) are found to be

$$\hat{p} \to \hat{p}_o z^2 \exp\left(-\frac{g_0 \mathcal{K}}{3z^3}\right) \quad \text{as} \quad z \to 0$$

and

$$\hat{p} \to \hat{p}_\infty z^{\frac{1}{3\gamma}} \exp\left(-\frac{3\gamma A_0 \mathcal{K}}{3\gamma - 2} z \frac{(3\gamma - 2)}{3\gamma}\right) \quad \text{as} z \to \infty \tag{5.1a,b}$$

where $\hat{p}_0$ and $\hat{p}_\infty$ are constants and the numbers g_0 and A_0 arise from the corresponding asymptotes for G given earlier. Higher order terms in these expressions can be found analytically, and, in fact, are needed for accurate numerical solutions to this eigenvalue problem for $\mathcal{C}$ and $\mathcal{K}$, the scaled relative wavespeed and the scaled wavenumber of the inviscid vorticity mode, discussed after briefly paying attention to the neutral case. There $\mathcal{C}$ is real and takes the value of G evaluated at the generalized inflection point which of course occurs where

$$GG_{zz} = 2G_z^2.$$

A numerical solution to (4.26) using a Runge-Kutta method shows that this occurs when $\xi = 1.661432$, where the new variable $\xi = \ell n z$ was introduced to 'stretch' the co-ordinate-scale for small z where G, and hence $\hat{p}$, vary rapidly. The resulting neutral value of the wavespeed is then given by

$$\mathcal{C} = -0.633318.$$

The corresponding real value of $\mathcal{K}$ is obtained from a numerical solution of (4.37) for all z with an appropriate treatment of the path of integration at the generalised inflection point (g.i.p.). The particular numerical procedure chosen to calculate this neutral wavenumber, and the complex eigenvalues $\mathcal{C}$ was to extend the line of integration into the complex-plane, taking a triangular contour around and below the g.i.p. The neutral value of $\mathcal{K}$ was calculated to be

$$\mathcal{K} = .477957$$

Figure (5.1) shows the growth rate $\mathcal{K}\mathcal{C}_i$ plotted against $\mathcal{K}$ we find that the maximum growth rate $\simeq .060918$ occurs at $\mathcal{K} \simeq .156100$ and that the growth rate goes to zero when the wavenumber goes to zero. In Figure (5.2) we show the eigenfunction of the most unstable mode, we note the exponential decay of the eigenfunction at both ends of the range of integration.

We shall now show how the small wavenumber structure of the strong interaction inviscid mode develops when the wavenumber tends to zero. In fact we simply give the structure corresponding to the first small wavenumber regime discussed in Section 3. Some discussion of the regimes encountered at even smaller wavenumbers will be given in the next section.

The small-$\mathcal{K}$ behaviour

Numerical solutions of the pressure-amplitude equation, (4.37), indicate that $\mathcal{C}$ grows as $\mathcal{K} \to 0$; exactly the same behaviour was found for the no shock problem studied in Section 3. However, in the latter, the leading order dependence on the wavenumber was indicated from the numerical solutions, whereas, in the present case, such guidance was not possible due to a complicated dependence of $\mathcal{C}$ on $\mathcal{K}$. Instead, the equation was studied analytically for small $\mathcal{K}$, and initial investigations suggested that

$$c \sim \left\{ \frac{(k^2)^{-4\epsilon} - 1}{4\epsilon} \right\}^{\frac{4}{7}}$$

as $k \to 0$. Here the parameter ϵ is a function of γ and is defined by

$$4\epsilon = 1 - \frac{4}{3\gamma} \tag{5.2}$$

and we have replaced $\mathcal{K}$, $\mathcal{C}$ by k, c respectively here and henceforth in this sub-section.

It follows from (5.2) that special attention is required for values of γ close to $\gamma = \frac{4}{3}$ and, as this coincides with the range of physically relevant values of the ratio of specific heat capacities, we solely consider the case of $|\epsilon| << 1$ in this section. We note that the suggested form of c is defined and continuous at $\gamma = \frac{4}{3}$ by appealing to "L'Hôpital's Rule". Below we outline the asymptotic regions and corresponding solutions required to resolve the leading order behaviour of c as $k \to 0$.

When z is very large, we have the WKB asymptote

$$\hat{P} \sim z^{\frac{1}{3\gamma}} \exp\left(-\frac{3\gamma A_0}{3\gamma - 2} k z^{\frac{3\gamma - 2}{3\gamma}} \right)$$

and we note that for smaller z this form breaks down in a 'turning-point' region corresponding to

$$z \sim k^{-\frac{3\gamma}{3\gamma - 2}} >> 1.$$

In this region we define

$$\hat{y} = k^{\frac{3\gamma}{3\gamma - 2}} z, \quad \hat{P} = \hat{P}_0(\hat{y}) + \cdots \tag{5.3a, b}$$

and, using the large-z asymptotes for G, we find that $\hat{P}_0$ satisfies

$$\hat{P}_{0\hat{y}\hat{y}} - A_0^2 \hat{y}^{-4\alpha} \hat{P}_0 = 0, \quad \alpha = \frac{1}{3\gamma}. \tag{5.4a,b}$$

This equation for $\hat{P}_0$ has an analytic solution involving the modified Bessel Function K, the required solution being

$$\hat{P}_0 = \bar{D}_0 \eta^\mu K_\mu(\frac{1}{2}\eta) \tag{5.5a}$$

where

$$\eta = 4A_0\mu\hat{y}^\nu, \quad \nu = 1 - 2\alpha \text{ and } \mu = \frac{1}{2\nu}. \tag{5.5b,c,d}$$

Here $\bar{D}_0$ is an arbitrary constant. We can investigate the small $\hat{y}$ behaviour of $\hat{P}_0$ by considering the limiting forms, for small arguments, of the modified Bessel functions. We find that

$$\hat{P}_0 = \bar{D}_0 \frac{\pi(1-\mu)}{\sin(\mu\pi)} 2^{2\mu-1}[1 + \frac{A_0^2\mu^2\hat{y}^{2\nu}}{(1-\mu)} - \frac{\Gamma(2-\mu)(A_0^2\mu^2)^\mu}{\Gamma(1-\mu)(1-\mu)}\hat{y} + \cdots] \tag{5.6}$$

as $\hat{y} \to 0$, the ordering of the second and third terms being dependent on the value of γ; we note that the corresponding powers of $\hat{y}$ (the indicial roots of the associated Frobenius solution) become equal when $\gamma = \frac{4}{3}$. Moreover, the coefficients of these terms are also singular when γ has this value (note that $\gamma = \frac{4}{3} \leftrightarrow \mu = 1$). Here Γ is the Gamma function.

That special attention is needed for values of γ near four-thirds is now apparent and, as mentioned earlier, it is exactly this range of γ that we are interested in, physically. Considering $\epsilon = \frac{1}{4} - \alpha$ to be small, we see that

$$\hat{P}_{0\hat{y}} \sim 2\bar{D}_0 A_0^2 \Big[(\frac{\hat{y}^{4\epsilon} - 1}{4\epsilon}) + 1 + O(\epsilon)\Big] \tag{5.7}$$

as $\hat{y} \to 0$. We note that $\hat{P}_{0\hat{y}}$ (and, in fact, $\hat{P}_0$) is defined, and moreover, continuous as $\epsilon - 0$. It is convenient to recast the last result in terms of z to ease matching to the next asymptotic region to be discussed. The result is that

$$\hat{P}_{0z} \sim 2\bar{D}_0 A_0^2 k^{\frac{1}{1-2\alpha}} \Big[k^{\frac{4\epsilon}{1-2\alpha}}(\frac{z^{4\epsilon} - 1}{4\epsilon}) + (\frac{k^{\frac{4\epsilon}{1-2\alpha}} - 1}{4\epsilon}) + 1\Big] \tag{45}$$

as $z \to 0$.

The solution for $\hat{P} = \hat{P}_0(\hat{y}) + \cdots$, will continue to be the leading order behaviour of $\hat{P}$ until contributions from the 'middle'-term (proportional to $\hat{P}_z$) become leading order. The

location of this next region of interest can be easily located, by analogy with the respective analysis of Section 3, as we expect $c >> 1$ as $k \to 0$. Here $z \sim c^{-1/4}$, using the small-z asymptote of G, and we expand

$$\hat{P} = 2\bar{D}_0[1 + k^2\delta_2^{3/2}\bar{P}(\bar{y}) + \cdots], \quad c = \hat{c}\delta_2 + \cdots \tag{5.9a,b}$$

where $\delta_2, = \delta_2(k;\epsilon)$, is a small parameter. The $\hat{P}$ form is implied from the $\hat{P}_0$ solution for small $\hat{y}$. The new, scaled normal variable, $\bar{y}$ is taken to be $O(1)$ and is defined by

$$z = \delta_2^{-1/4}\bar{y} \ (<< 1). \tag{5.10}$$

Substituting into the pressure-amplitude equation, (4.37), yields the equation satisfied by $\bar{P}$

$$\bar{P}_{\bar{y}\bar{y}} + \frac{8g_0}{\bar{y}(g_0 + \hat{c}\bar{y}^4)}\bar{P}_{\bar{y}} = \frac{g_0^2}{\bar{y}^8} \tag{5.11}$$

where g_0 arises from the small-z asymptote of G. This can easily be integrated to give

$$\bar{P}_{\bar{y}}(\bar{y}) = (\hat{c} + \frac{g_0}{\bar{y}^4})^2\Big(\int_\infty^{\bar{y}} \frac{g_0^2 d\bar{y}}{(\hat{c}\bar{y}^4 + g_0)^2} + D_1\Big), \tag{5.12}$$

with D_1 an arbitrary constant to be determined by matching with the previous region. As $\bar{y} \to \infty$ we see that $\bar{P}_{\bar{y}} \to D_1\hat{c}^2$, thus $\bar{P}_z \to D_1\hat{c}^2\delta_2^{1/4}$ and matching with (5.8) gives

$$k^2 D_1\hat{c}^2\delta_2^{7/4} = A_0^2 k^{\frac{4\epsilon}{1-2\alpha}}\Big[\Big(\frac{k^{\frac{4\epsilon}{1-2\alpha}} - 1}{4\epsilon}\Big) + 1\Big],$$

at leading order. We choose $D_1 = -A_0^2\hat{c}^{-2}$ and this determines the size of c for small k

$$\delta_2^{7/4} = -\Big[\frac{(k^{\frac{2}{1+4\epsilon}})^{-4\epsilon} - 1}{-4\epsilon}\Big] - k^{-\frac{8\epsilon}{1+4\epsilon}} \tag{5.13}$$

Taking the limiting value as $\epsilon \to 0$, we have that when $\gamma = \frac{4}{3}$

$$\delta_2^{7/4} = -\ln k^2 - 1 \quad >> 1 \tag{5.13}$$

recalling that $\ln x \to -\infty$ as $x \to 0$; the choice of $D_1 < 0$ ensuring that δ_2 is real and we allow $\hat{c}$ to be complex. When ϵ is small we see that δ_2 is large and has the form suggested at the start of this section. Thus δ_2, as given by (5.13), leads us to conclude that, for the physically realistic values of γ around four-thirds, the scaled, relative wavespeed c

increases as the scaled wavenumber k decreases, this growth having logarithmic magnitude in contrast to the much faster algebraic growth found in the no-shock analysis presented in Section 3. We note that the corresponding frequency, proportional to ck, tends to zero as k decreases. The $k-$ dependence of c, for $k \to 0$, can be deduced in a similar fashion for other values of γ, and we note that, mathematically, the no-shock result of Section 3 is the limiting case $\gamma \to \infty$.

All that remains now is to determine $\hat{c}$ and this is easily deduced by introducing a further region where $z \sim k^{1/3} << 1$. The details are identical to those of Region IV in Section 3; again we find we need $\bar{P}_{\bar{y}} \to 0$ as $\bar{y} \to 0$, resulting in an expression for $\hat{c}$

$$\int_0^\infty \frac{g_0^2 d\bar{y}}{(\hat{c}\bar{y}^4 + g_0)^2} + \frac{A_0^2}{\hat{c}^2} = 0$$

which can be solved for complex $\hat{c}$; after an elementary contour integration and a little manipulation we obtain

$$\hat{c} = -\left(\frac{8\sqrt{2}A_0^2}{3\pi g_0^{1/4}}\right)^{\frac{4}{7}} \exp(-\frac{3i\pi}{7}) \tag{5.14}$$

which corresponds to to an unstable mode of (4.37).

Thus we have obtained the structure of the vorticity mode in the strong interaction region at small values of the wavenumber. We postpone any further discussion of our results until the following section.

6 Discussion

We have investigated the instability of flat plate hypersonic boundary layers to the vorticity mode of instability. This inviscid mode is associated with the generalized inflection point of the basic flow and is thought to be the most dangerous mode of instability of a high Mach number flow. When the mode is neutral the wave propagates downstream with the speed of the fluid at the generalized inflection point. At wavenumbers smaller than the neutral value the mode is unstable and the growth rate attains it's maximum value at a finite value of the wavenumber. In the small wavenumber limit the growth rate approaches zero and for the non-interactive boundary layer at sufficiently small wavenumber the vorticity mode spreads out towards the lower boundary and reduces to an acoustic mode at a countable infinite set of wavenumbers. We believe that a similar process happens in the strong interaction case since there the acoustic mode is correctly described by a quasi-parallel theory there. We did not pursue that calculation here because it would be essentially unchanged from that of Section 3 except that it would be made somewhat more complicated by the necessity of treating the case $\gamma = 4/3$ as a special case in the strong interaction zone.

We believe that the results we have presented in Section 4 are the first which show the effect of a leading edge shock on any form of hydrodynamic instability. Interestingly enough the shock does not have a direct influence on the vorticity mode; thus the main effect of the shock is to restructure the boundary layer in the leading edge region and thereby influence the susceptibility of the flow to inviscid disturbances.

The vorticity mode eigenvalue problem was formulated in the interactive region along the plate at $O(1)$ values of x. However to the authors' knowledge the basic flow in this regime has not yet been calculated; the numerical problem was set up by Bush (1966) but is sufficiently difficult to have remained unsolved. Thus we were unable to solve the eigenvalue problem in this regime and therefore choose to consider the strong interaction regime where a similarity solution for the basic state is available. An alternative to that limit would have been to consider the weak-interaction problem, Bush and Cross (1967), where a different similarity structure holds. We choose to concentrate on the strong interaction limit because the growth rates there are bigger and if the flow is indeed unstable there the stability of the flow further downstream is possibly of less relevance.

Unfortunately we are unaware of any experimental observations or other theoretical work which we could compare with our results for the strong interaction regime.

In Section 3 we showed how the acoustic inviscid mode emerges from the small wavenumber description of the vorticity mode. Again it is not possible for us to compare our work with that of previous authors since it appears that the finite Mach number calculations available, mostly due to Mack, have either being carried out using a Chapman viscosity law or a combination of Sutherland's and Chapman's law. In fact Mack's calculations were carried out using a combination of the different laws so as to efficiently model the viscosity-temperature structure of the fluid. The fact that the calculations of Cowley and Hall(1988) and Smith and Brown (1989) agree so well with Mack's calculations suggests that over the part of the flow where instability took place Chapman's law was being used; in the case of the vorticity mode this is clearly a bad approximation because the mode locates itself in the layer where the basic temperature field varies rapidly.

REFERENCES

Balsa, T.F., & Goldstein, M.E. 1989 On the instabilities of supersonic mixing layers: a high Mach number asymptotic theory. Submitted to *J.Fluid Mech.*

Brown, S.N., & Stewartson, K. 1975 A non-uniqueness of the hypersonic boundary layer. *Q.J.A.M*, **XXVIII**, 75-90.

Bush, W.B. 1966 Hypersonic strong interaction similarity solutions for flow past a flat plate. *J.Fluid Mech.* **25**, 51-64.

Bush, W.B., & Cross, A.C. 1967 Hypersonic weak interaction similarity solutions for flow past a flat plate. *J.Fluid Mech.* **29**, 349-359.

Cowley, S.J. & Hall, P. 1988 On the instability of flow past a wedge. *ICASE REPORT* **88-72** and to appear in *J.Fluid Mech.*.

Hall, P. & Fu, Y. 1989 Görtler vortices at hypersonic speeds. *Theor.Comp.Fluid Mech.* **1**, 125-134.

Jackson, T.L. & Grosch, C.E. 1989 Inviscid spatial instability of a compressible mixing layer. *J.Fluid Mech* **208** 609-638.

Lee, R.S. & Cheng, H.K. 1969 On the outer edge problem of a hypersonic boundary layer. *J.Fluid Mech.* **38**, 161-179.

Lees, L. & Lin, C.C. 1946 Investigation of the stability of the laminar boundary layer in a compressible fluid. *NACA Tech. Note* No. 1115

Luniev, V.V. 1959 On the similarity of hypersonic viscous flows around slender bodies *PMM* **23**, 193-197.

Mack, L.M. 1984 Boundary-layer linear stability theory. In *Special Course on Stability and Transition of Laminar Flow.* AGARD Rept 709.

Mack, L.M. 1987 Review of linear compressible stability theory. In *Stability of Time Dependent and Spatially Varying Flows*, eds. D.L. Dwoyer &. M.Y. Hussaini. Springer-Verlag.

Papageorgiou, D.T. 1989 Linear instability of supersonic plane wakes. *ICASE REPORT* **89-66**.

Reshotko, E. 1976 Boundary-layer stability and transition. *Ann. Rev. Fluid Mech.* **8**, 311-350.

Seddougui, S.O., Bowles, R.I. & Smith, F.T. 1989 Surface-cooling effects on compressible boundary layer instability. *ICASE REPORT* **89-95**.

Smith, F.T. 1979a On the non-parallel flow stability of the Blasius boundary layer. *Proc. R. Soc. Lond.* **A366**, 91.

Smith, F.T. 1979b Nonlinear stability of boundary layers for disturbances of various sizes. *Proc. R. Soc. Lond.* **A368**, 573 (also corrections 1980, **A371**, 439-440).

Smith, F.T. 1989 On the first-mode instability in subsonic, supersonic or hypersonic boundary-layers. *J.Fluid Mech* **198** 127-154.

Smith, F.T. & Brown, S.N. 1989 The inviscid instability of a Blasius boundary layer at large values of the Mach number. *J.Fluid Mech.* submitted for publication.

Stewartson, K., 1964. *Theory of laminar boundary layers in compressible fluids.* Oxford University Press.

Stewartson, K. 1955 On the motion of a flat plate at high speed in a viscous compressible fluid - II. Steady motion. *J. Aero. Sci.* **22** 303-309.

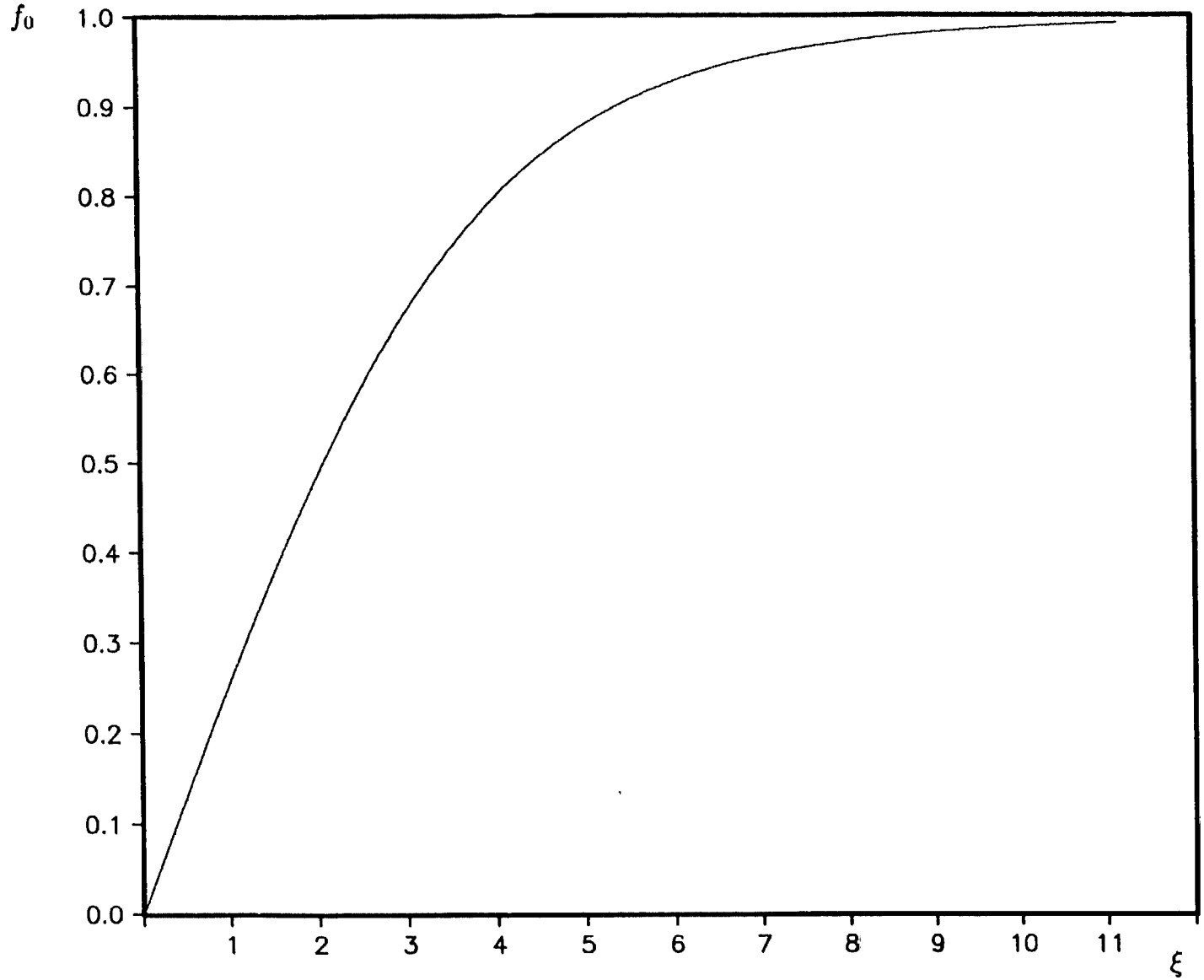

Figure (2.1a) The solution of the wall layer equation (2.8a) for the adiabatic case $T_s = 1$ with $\gamma = 1.4$.

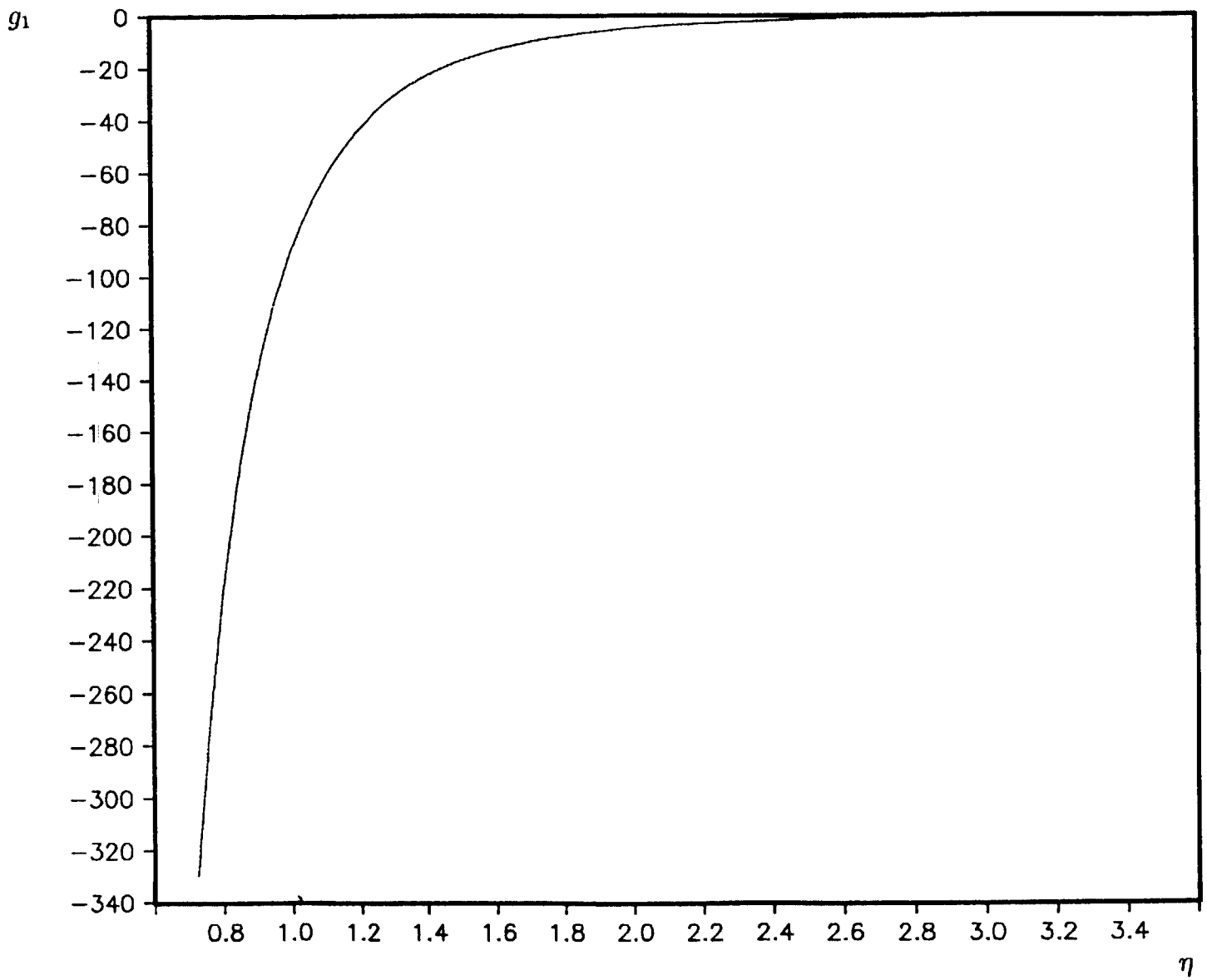

Figure (2.1b) The solution of the transition layer equation (2.10a) for the adiabatic case $T_i = 1$ with $\gamma = 1.4$..

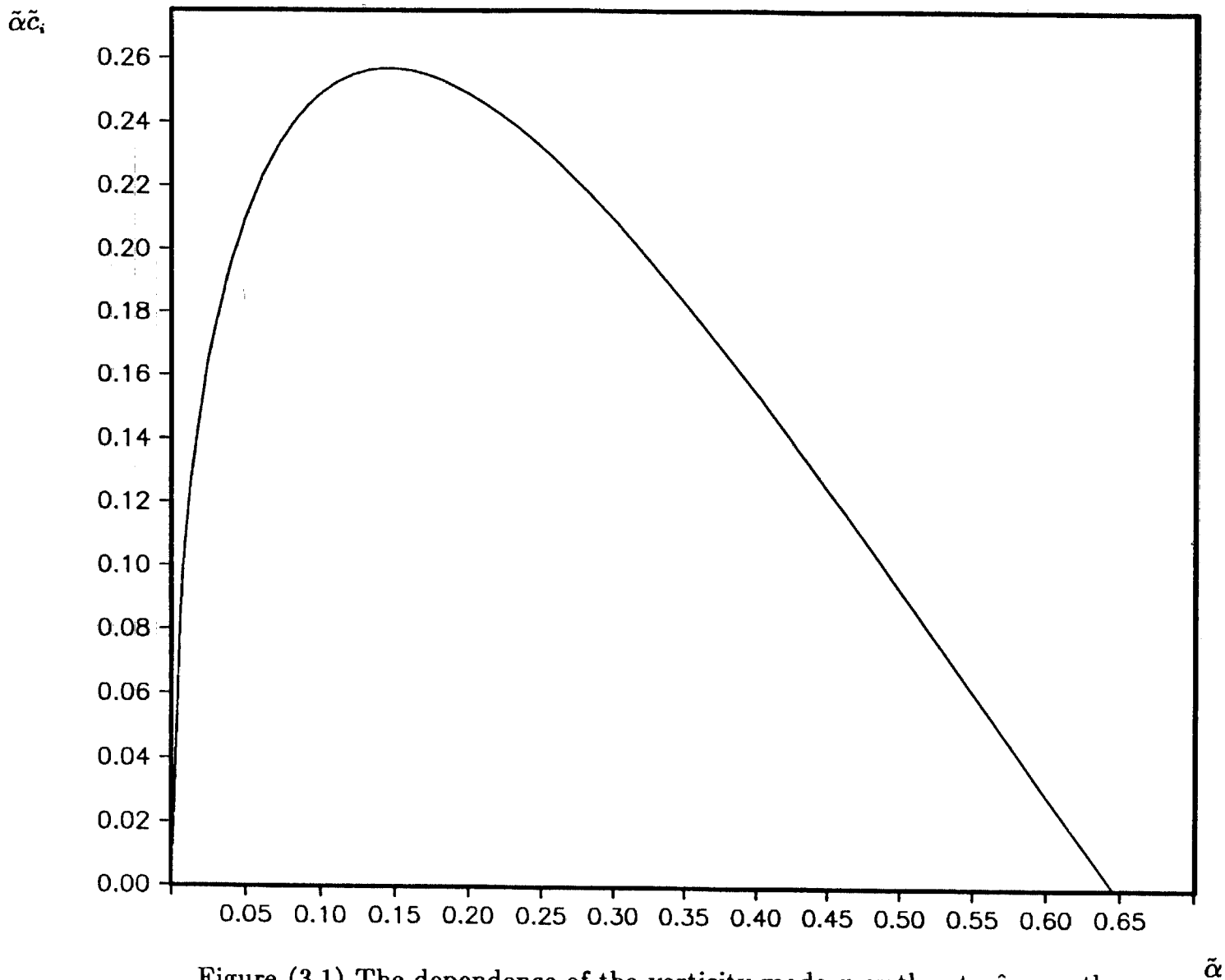

Figure (3.1) The dependence of the vorticity mode growth rate $\hat{\alpha}c_i$ on the wavenumber $\hat{\alpha}$.

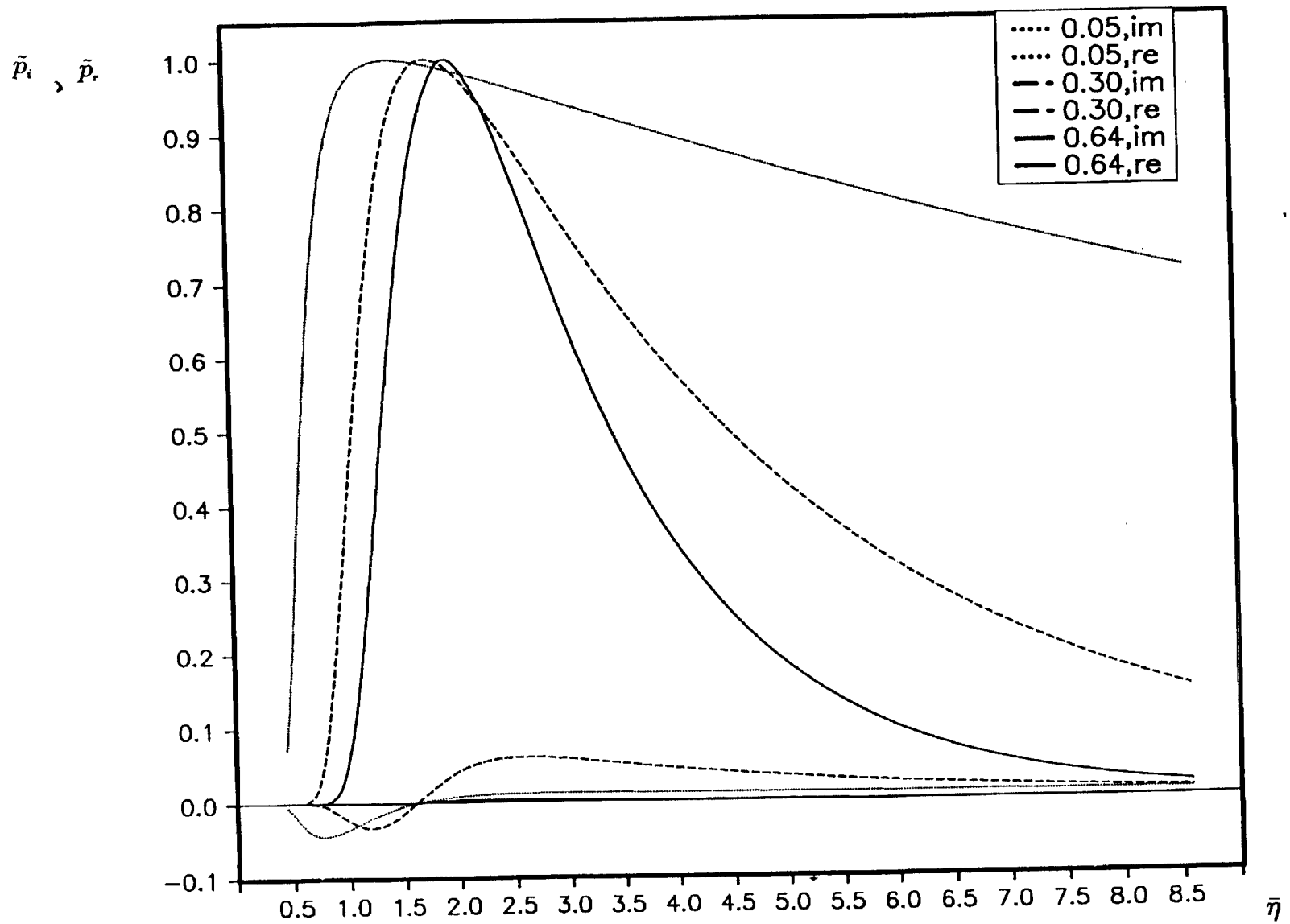

Figure (3.2) The vorticity mode eigenfunction at different values of the wavenumber.

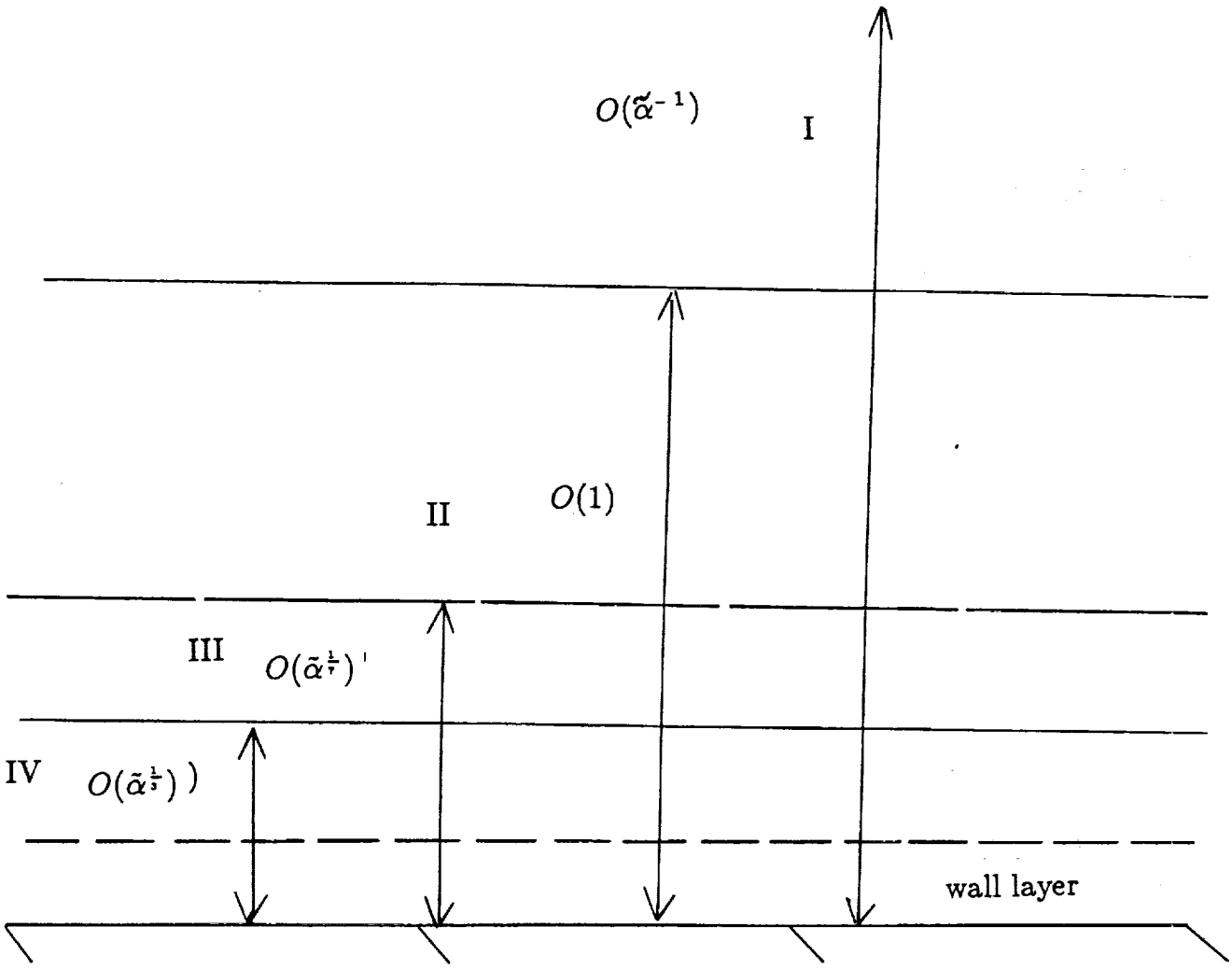

Figure (3.3) The different regions which emerge in the small $\hat{\alpha}$ limit.

Figure (3.4) The first three acoustic mode eigenfunctions. Modes 1,2,3 have 0,1,2 zeros in $(0, \infty)$ respectively.

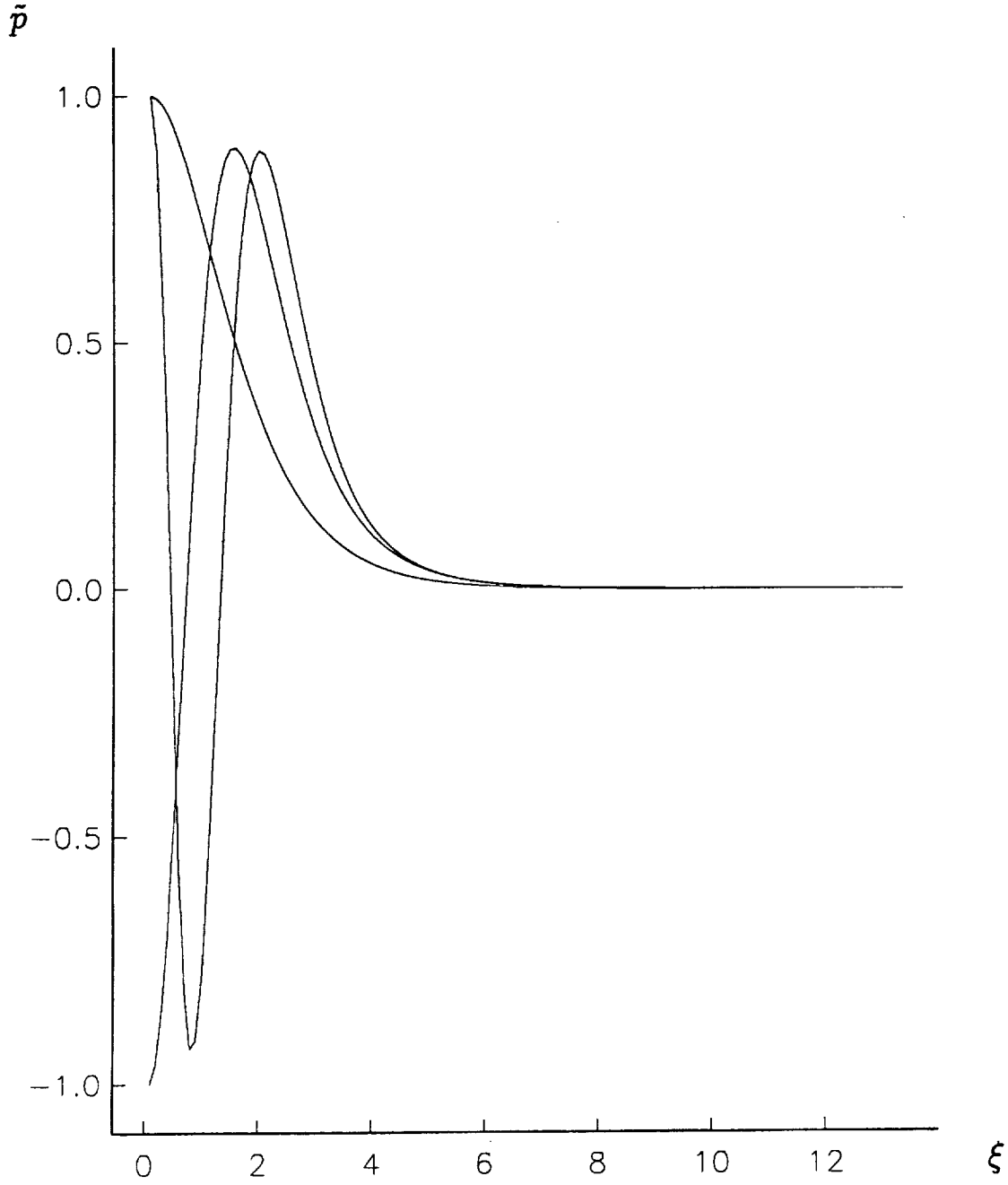

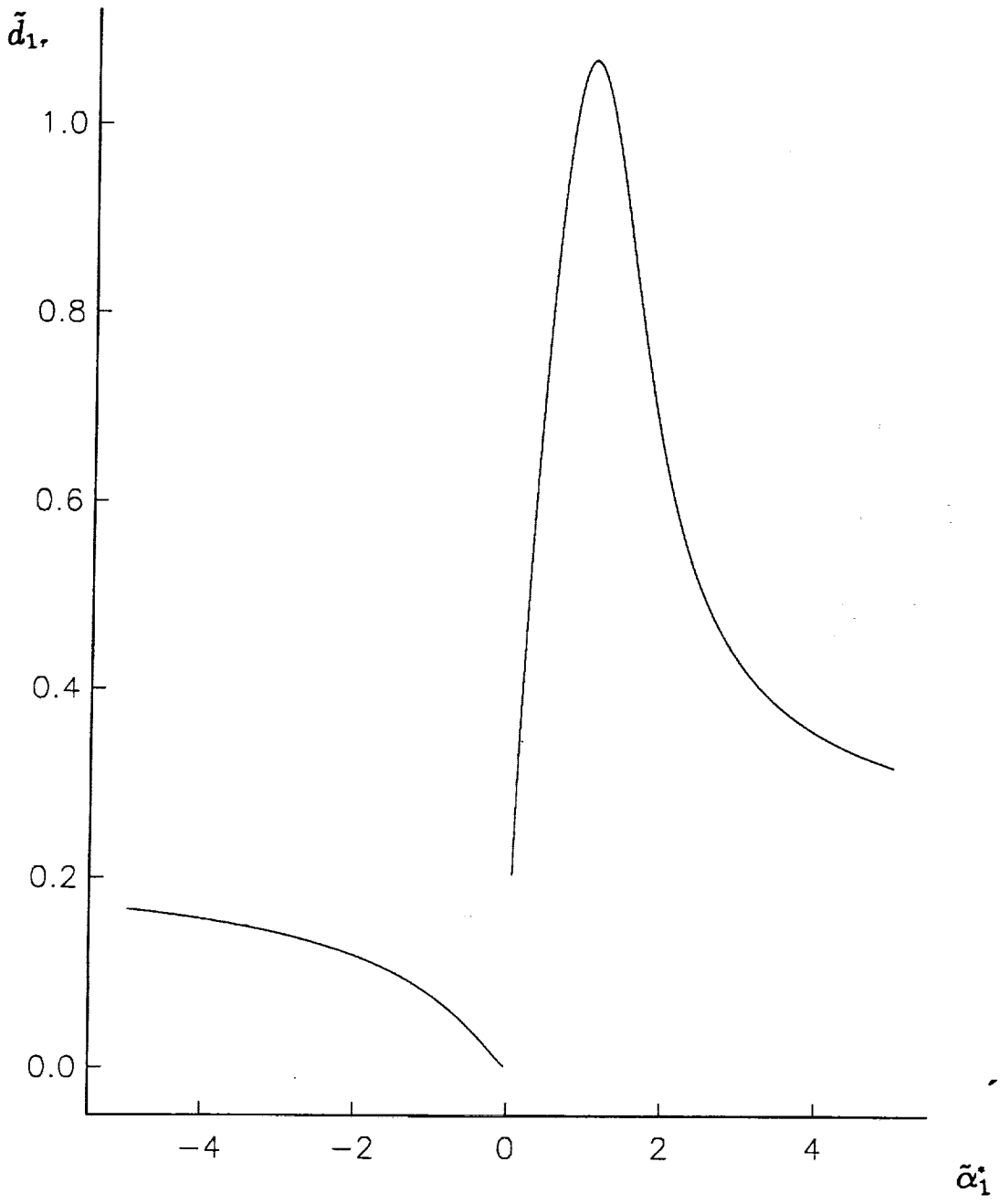

Figure (3.5a) The real part of the solution of (3.17) for $-5 < \tilde{\alpha}_1^* < 5$.

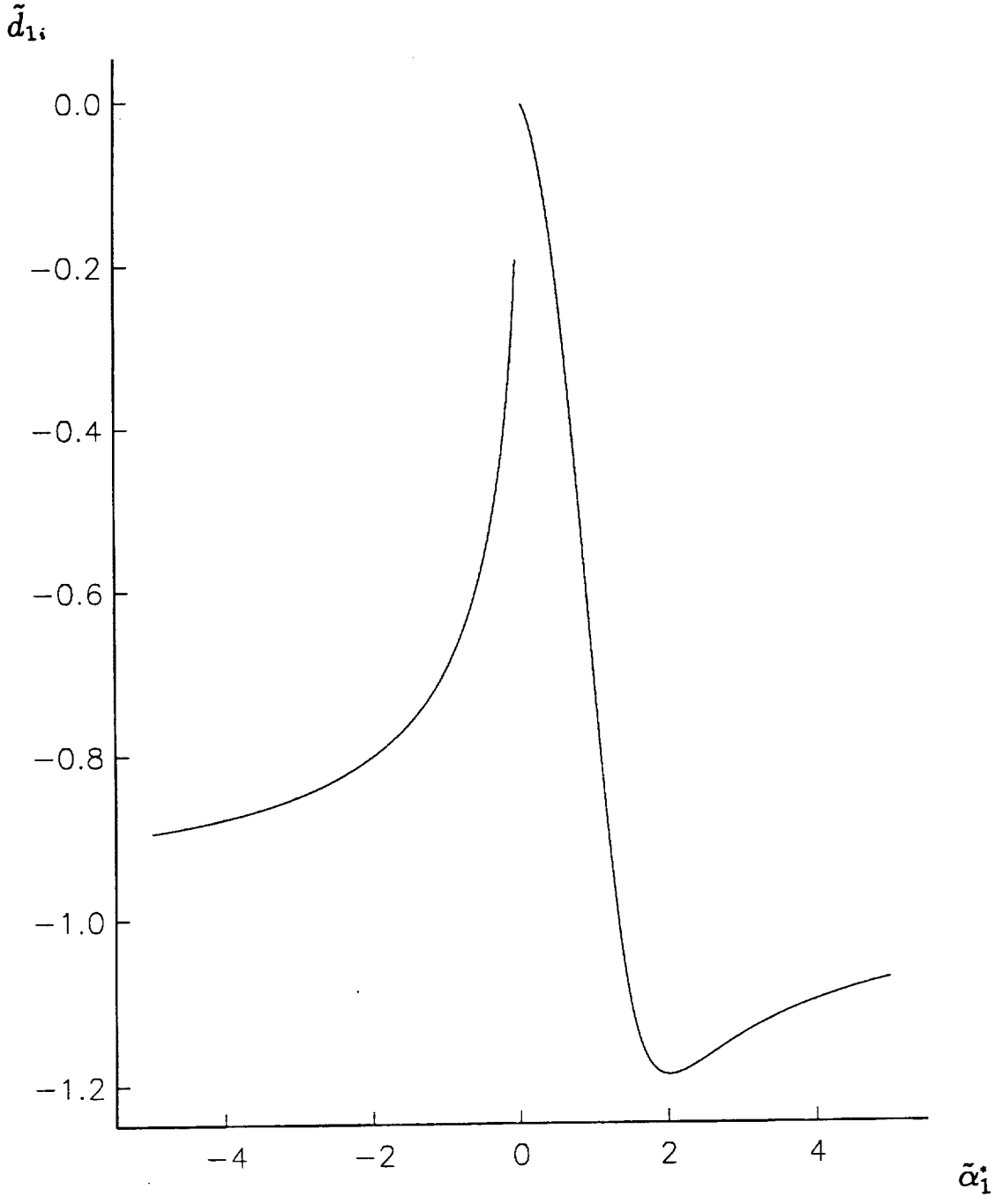

Figure (3.5b) The imaginary part of the solution of (3.17) for $-5 < \tilde{\alpha}_1^* < 5$.

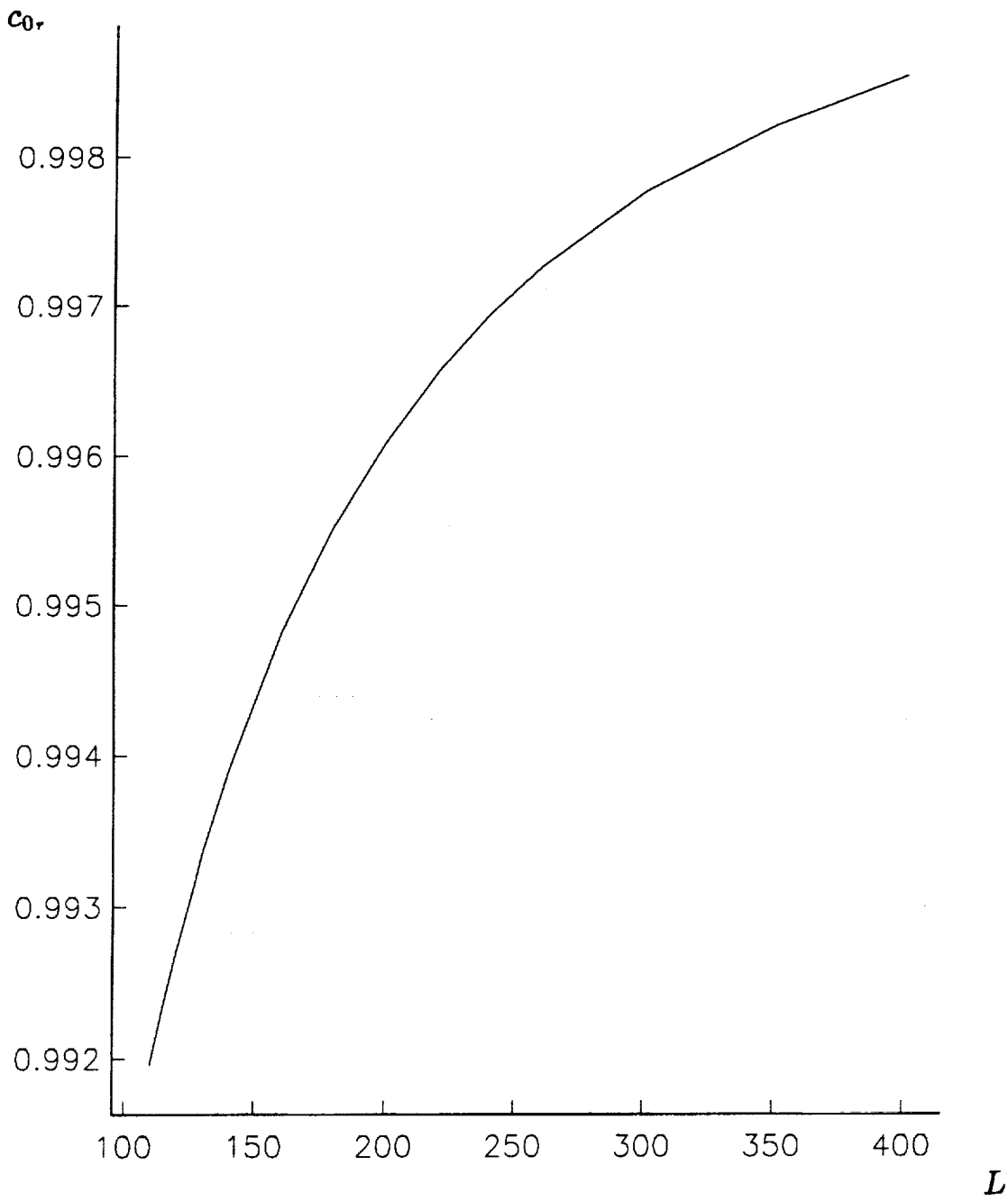

Figure (3.6a) The real part of the wavespeed c_0 as a function of L for $100 < L < 500$ and the case of an insulated wall.

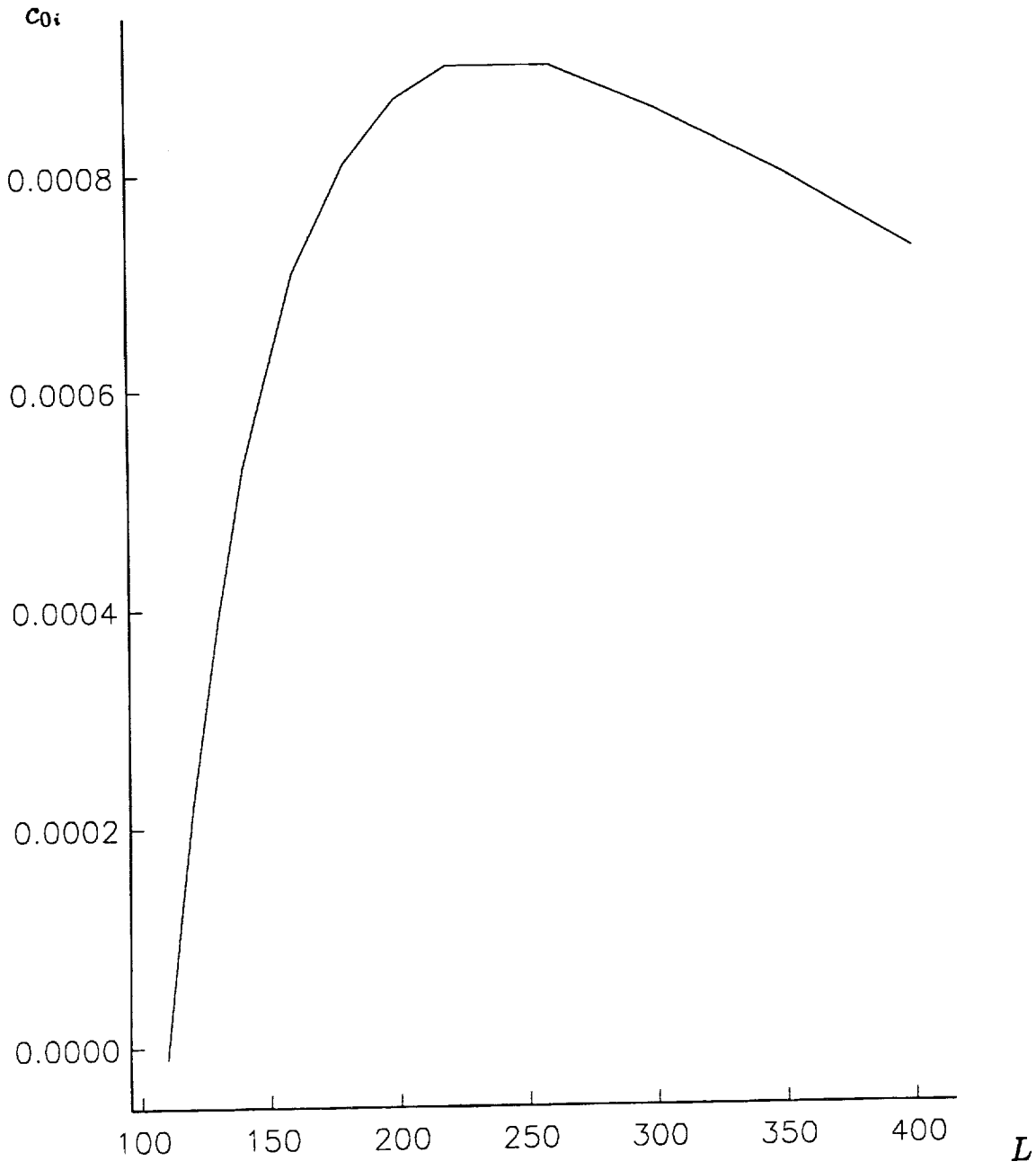

Figure (3.6b) The imaginary part of the wavespeed c_0 as a function of L for $100 < L < 500$ and the case of an insulated wall

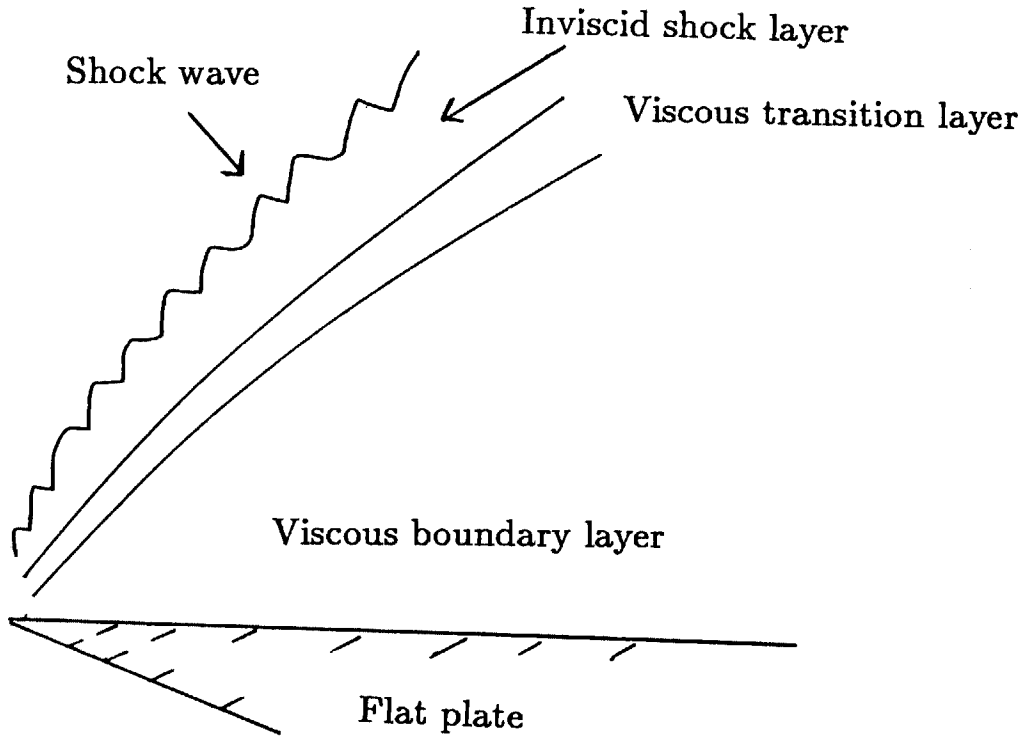

Figure (4.1) The different parts of the flow field in the hypersonic limit.

Figure (5.1) The growth rate of the vorticity mode in the strong interaction region.

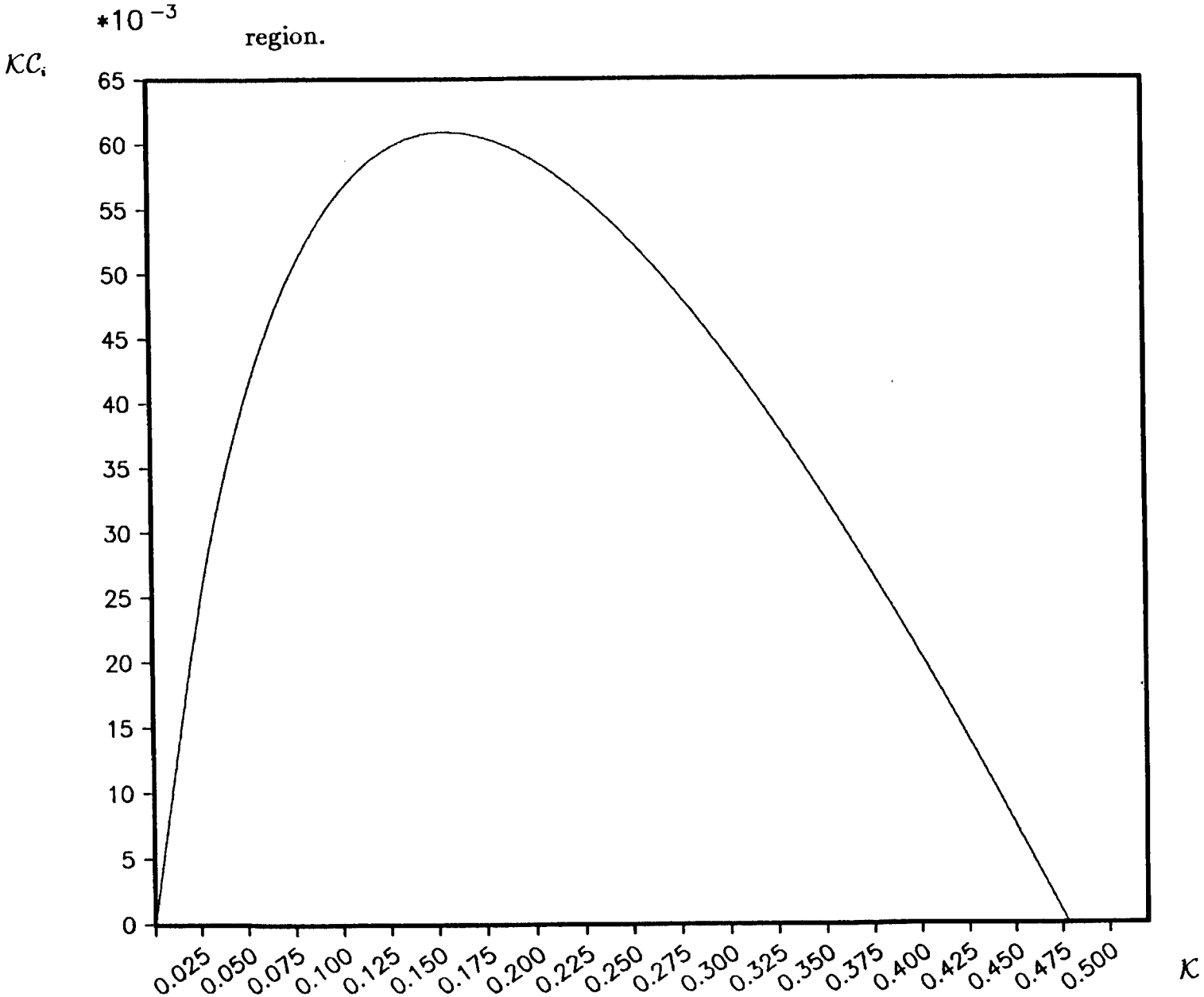

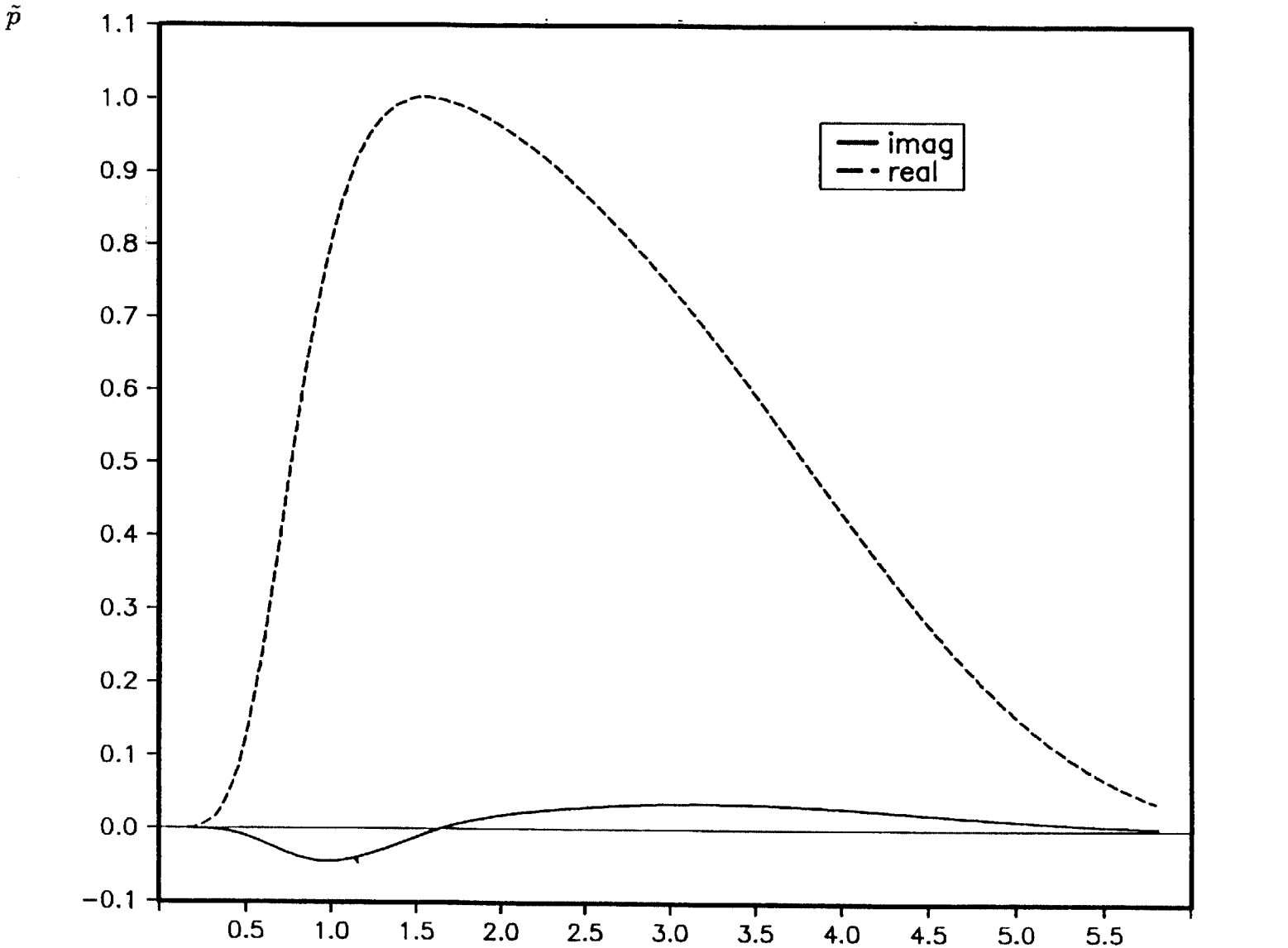

Figure (5.2) The eigenfunction of the most dangerous mode in the strong interaction limit.

NASA
National Aeronautics and Space Administration

Report Documentation Page

1. Report No.	2. Government Accession No.	3. Recipient's Catalog No.
NASA CR-182051 ICASE Report No. 90-40		

4. Title and Subtitle

ON THE INSTABILITY OF HYPERSONIC FLOW PAST A FLAT PLATE

5. Report Date

May 1990

6. Performing Organization Code

7. Author(s)

Nicholas Blackaby
Stephen Cowley
Philip Hall

8. Performing Organization Report No.

90-40

10. Work Unit No.

505-90-21-01

9. Performing Organization Name and Address

Institute for Computer Applications in Science and Engineering
Mail Stop 132C, NASA Langley Research Center
Hampton, VA 23665-5225

11. Contract or Grant No.

NAS1-18605

13. Type of Report and Period Covered

Contractor Report

12. Sponsoring Agency Name and Address

National Aeronautics and Space Administration
Langley Research Center
Hampton, VA 23665-5225

14. Sponsoring Agency Code

15. Supplementary Notes

Langley Technical Monitor:
Richard W. Barnwell

Final Report

Submitted to J. Fluid Mechanics

16. Abstract

The instability of hypersonic boundary-layer flows over flat plates is considered. The viscosity of the fluid is taken to be governed by Sutherland's law, which gives a much more accurate representation of the temperature dependence of fluid viscosity at hypersonic speeds than Chapman's approximate linear law; although at lower speeds the temperature variation of the mean state is less pronounced so that the Chapman law can be used with some confidence. Attention is focussed on the so-called "vorticity" mode of instability of the viscous hypersonic boundary layer. This is thought to be the fastest growing inviscid disturbance at hypersonic speeds; it is also believed to have an asymptotically larger growth rate than any viscous or centrifugal instability. As a starting point we investigate the instability of the hypersonic boundary layer which exists far downstream from the leading edge of the plate. In this regime the shock that is attached to the leading edge of the plate plays no role, so that the basic boundary layer is non-interactive. It is shown that the vorticity mode of instability of this flow operates on a significantly different lengthscale than that obtained if a Chapman viscosity law is assumed (see Smith and Brown, 1989). In particular, we find that the growth rate predicted by a linear viscosity law overestimates the size of the growth rate by $O(M^2)$. Next, the development of the vorticity mode as the wavenumber decreases is described, and it is shown that acoustic modes emerge when the wavenumber has decreased from it's O(1) initial value to $O(M^{-\frac{1}{2}})$. Finally, the inviscid instability of the boundary layer near the leading edge in the interaction zone is discussed and particular attention is focussed on the strong interaction region which occurs sufficiently close to the leading edge. We find that the vorticity mode in this regime is again unstable, and that it is concentrated in the transition layer at the edge of the boundary layer where the temperature adjusts from its large, $O(M^2)$, value in the viscous boundary layer, to its O(1) free stream value. The existence of the shock indirectly, but significantly, influences the instability problem by modifying the basic flow structure in this layer.

17. Key Words (Suggested by Author(s))	18. Distribution Statement
instability, transition, hypersonic	02 - Aerodynamics 34 - Fluid Mechanics and Heat Transfer Unclassified - Unlimited

19. Security Classif. (of this report)	20. Security Classif. (of this page)	21. No. of pages	22. Price
Unclassified	Unclassified	52	A04